Check for updates

# A new generation of energy storage electrode materials constructed from carbon dots

Ji-Shi Wei, [ID] †[a] Tian-Bing Song,†[a] Peng Zhang,[a] Xiao-Qing Niu,[a] Xiao-Bo Chen [ID] [b] and Huan-Ming Xiong*[a]

Carbon dots (CDs), an emerging class of carbon materials, hold a promising future in a broad variety of engineering fields owing to their high diversity in structure, composition and properties. Recently, their potential applications have spanned from bio-imaging, fluorescent probing and catalysis, to energy storage fields, in particular as materials in the key components of electrochemical energy storage devices. The state-of-the-art research work has revealed that CD-based or modified electrodes exhibit profound improvement in all key functions, such as coulombic efficiency, cycling life, enlarging capacity, *etc.*, in comparison to traditional electrodes. The improvement in all these properties can be realized by introducing a small quantity of CDs to the traditional electrode systems. A comparative optimization in this regard, however, requires incorporation of more carbon nanotubes (CNTs) or graphene or other carbon-based materials, indicating that CD-incorporated electrode materials would maintain their energy density more efficiently. This review will summarize the progress to date in the design and preparation of CD-incorporated energy storage devices, including supercapacitors, Li/Na/K-ion batteries, Li–S batteries, metal–air batteries and flow batteries, and elaborate on the influence of these unique structures and rich properties of CDs on the electrochemical performance of the resulting electrodes and devices. Consequently, the specific functions and the novel working mechanisms of CD-modified electrodes for energy storage units will be discussed, aiming at providing new insights for guidance for design and manufacturing of the next generation of electrode materials for high-performance energy storage.

[a] *Department of Chemistry and Shanghai Key Laboratory of Molecular Catalysis and Innovative Materials, Fudan University, Shanghai 200433, P. R. China. E-mail: hmxiong@fudan.edu.cn*
[b] *School of Engineering, RMIT University, Carlton, VIC 3053, Australia*
† These authors contributed equally to this review.

## 1. Introduction

Carbon materials play a crucial role in the fabrication of electrode materials owing to their high electrical conductivity, high surface area and natural ability to self-expand.[1] From zero-dimensional

**Ji-Shi Wei**

*Dr Ji-Shi Wei was awarded his BSc from Henan Normal University in July 2014, and PhD from Fudan University in June 2019, respectively. Now, he will join the National University of Singapore (NUS) as a research fellow for his postdoctoral training. His PhD research work covering super-capacitor electrode materials, bi-functional oxygen reaction electro-catalysts, nickel–zinc battery electrode materials and preparation processes of CDs was conducted under the supervision of Prof. Huan-Ming Xiong.*

**Tian-Bing Song**

*Mr Tian-Bing Song received his MS degree from Shanghai University of Electric Power in June 2019. He is now a PhD candidate of the Department of Chemistry under the supervision of Prof. Huan-Ming Xiong at Fudan University. His research projects focus on the preparation, characterization and optimization of CDs to fabricate electrodes for high-performance electrochemical energy storage.*

carbon dots (CDs), one-dimensional carbon nanotubes, two-dimensional graphene to three-dimensional porous carbon, carbon materials exhibit a great diversity in dimension, structure and size as listed in Table 1.[2–4] In recent years, all categories of carbon materials have been extensively explored as electrode materials for various energy storage devices. For instance, graphite anodes have been commercialized in lithium ion batteries (LIBs) due to the low cost and high abundance of graphite.[5] Hard carbon is also a competitive anode material for sodium ion batteries (SIBs).[6] Over the past few years many attempts have been made to explore electrode materials modified using CNTs and graphene with optimized electrical conductivity and specific surface area.[7] It is evident that each new carbon material has secured a spot on the stage centre in terms of high-performance electrochemical energy storage. As shown in Table 1, CDs stand out among the carbon family members in terms of smaller size, abundant surface groups, homogeneous dispersion, adjustable composition and structure, facile fabrication and low cost.

As a new derivative member of the carbon family, CDs–carbon nanoparticles with diameters not larger than 10 nm – have attracted great attention since 2004.[14] It has been well recognized that CDs exhibit high luminescence, good solubility, chemical stability, biocompatibility and abundant surficial groups, and demonstrate great potential for a broad range of practical applications spanning from bio-imaging and bio-sensing to photocatalysis, solar cells and LEDs.[15] Moreover, for next generation energy storage materials, CDs can also play a promising role. According to the statistical data, as listed in Fig. 1a, research on CD-based electrode materials has been booming since 2013.[16] In the beginning, a few pioneering research groups made some prospective achievements, using CDs to construct electrode materials in different energy storage devices, such as Li/Na/K ion batteries,[17] Li–S batteries[18] and supercapacitors,[19] etc. By far, some key functions of CDs in electrodes have been identified (Fig. 1b): (1) improving coulombic efficiency (Li/Na/K ion batteries); (2) extending the cycling life span; (3) offering abundant surficial functional groups for faradaic reactions (supercapacitors); (4) enhancing interfacial wettability; and (5) promoting ORR/OER (metal–air batteries). As for the related reviews of CDs, previous articles

*Mr Peng Zhang obtained his BSc in July 2015 and MSc in January 2019 both from Fudan University. His research focused on oxygen reaction electrocatalysis and preparation of CDs, supervised by Prof. Huan-Ming Xiong. He will join The University of Sydney, Australia, in late 2019 to commence his PhD training.*

**Peng Zhang**

*Ms Xiao-Qing Niu received her BSc in 2013 and MSc in 2016 from Henan Normal University. She is currently a PhD candidate under the supervision of Prof. Huan-Ming Xiong at Fudan University. Her research interests focus on designed synthesis of carbon dots and their optical properties.*

**Xiao-Qing Niu**

*Dr Xiao-Bo Chen was awarded a PhD in Materials Science and Engineering from Deakin University in 2010 and now is a Senior Research Fellow in the School of Engineering, RMIT University. His research is multidisciplinary and spans from chemistry and materials science through to corrosion, electrochemistry and biomaterials, and shows promise in benefitting the wider community. Dr Chen's research aims to provide the surface functional characteristics of both structural and functional materials to satisfy a large range of engineering applications in automotive, 3C and biomedical industries.*

**Xiao-Bo Chen**
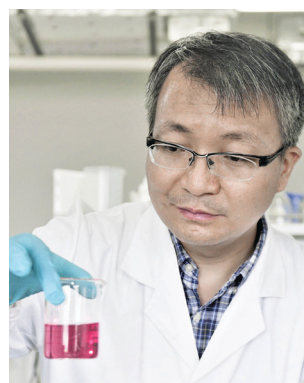
*Prof. Huan-Ming Xiong received his BSc in 1999 and PhD in 2004 from Jilin University, respectively. Then he joined the Department of Chemistry in Fudan University as a lecturer. He was promoted to an associate professor in 2007, a doctor adviser in 2009 and a full professor in 2012, respectively. During 2008–2009, he worked as an Alexander von Humboldt fellow at the Max-Planck Institute of Colloids and Interfaces in Germany. His research focuses on multifunctional hybrid nanomaterials, which can be applied in electrochemical energy storage and biomedical treatment. He has published more than 60 SCI papers, with a total citation number of over 5000 and an H index of 38.*

**Huan-Ming Xiong**

**Table 1**  Basic features of a number of representative carbon materials

| Materials | Dimension | Size | Defects/surficial groups[a] | Controllable synthesis[a] | Cost[a] |
|---|---|---|---|---|---|
| CDs | 0-D | ~10 nm | Abundant | Good | Low |
| CNTs | 1-D | 2–50 nm (D.) | Moderate | Average | High |
| Graphene | 2-D | From nanometer to micrometer scale | Moderate | Average | Moderate |
| Porous carbon | 3-D | From nanometer to micrometer scale | Moderate | Average | Low (activated carbon)/ high (templated carbon) |

[a] Note: these results are according to the related literature and market fluctuation.[8–13]



**Fig. 1**  (a) Literature concerning CDs as energy storage materials in Web of Science Core Collection, search date: 2019 July 23. Timespan: 2013–2019; (b) various energy storage systems employing CDs as electrode materials.
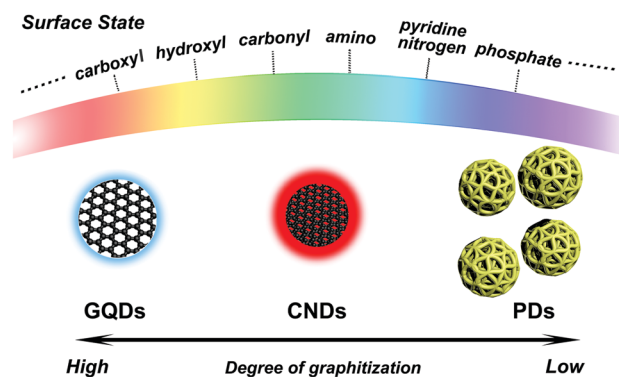


**Fig. 2**  Schematic diagram of the classification and structure of CDs.

mainly focused on their applications in syntheses, fluorescence analyses, bio-sensors, optoelectronic devices, *etc.* To our knowledge, this is the first time electrochemical energy storage research studies based on CDs have been summarized in a review article.

In the following sections, a brief introduction regarding definitions of CDs will be made, involving microstructures and physical–chemical properties of different types of CDs. Then, the applications and functions of CDs for various electrochemical energy storage-related devices will be reviewed. Finally, perspectives will be provided for the opportunities of optimizing CDs as a future generation of energy storage materials.

## 2. Basic features of carbon dots

### 2.1 Definition and structures of CDs

Carbon dots are a class of spherical carbon nanoparticles with diameters usually less than 10 nm, which include graphene quantum dots (GQDs), carbon nanodots (CNDs), and carbonized polymer dots (PDs). The structure of CDs consists of two parts: core and surface. For the core part, GQDs exhibit a graphitic nanocrystal structure, CNDs consist of amorphous carbon together with embedded $sp^2$-hybridized crystalline regions, while cross-linked linear polymers or monomers are the features of PDs (Fig. 2).[20] In addition to the core structures, surface states also have a profound effect on the properties of CDs, which are determined by surface functional groups, defects, edges, *etc.*[21] Compared with the core structures, surface states have a great influence on CDs more directly, especially the photoluminescence properties.

As for the electrochemical applications, CDs have at least four advantages. Firstly, CDs can increase electrical conductivity through their conductive graphitized cores and accelerate ion transport through their interfacial edges and ion diffusion paths, respectively. Secondly, CDs with rich functional groups and various defects can provide abundant absorption sites that effectively restrain the dissolution of electrode materials and buffer the volumetric expansion. Thirdly, the good dispersibility of CDs helps them distribute into composite materials homogeneously, which ensures the uniformity and stability of electrodes. Finally, the small size and abundant surface functional groups of CDs can enhance the surface wettability of electrode materials, so as to facilitate the electrochemical reactions between electrodes and electrolytes.

### 2.2 Synthesis of CDs

"Top-down" and "bottom-up" approaches are the main chemical preparation techniques for CDs. In general, through the former methods, CDs are usually obtained from a larger carbon structure, like graphite powders. The specific methods include acidic oxidation–exfoliation, electrochemical exfoliation, microwave approaches, *etc.* In these processes, original bulk carbon is divided into ultra-fine pieces, which leads to fluorescence properties. Advantages of these preparative routes are clear structures of final products and large-scale production with controllable conditions.[20] For example, Kang's group reported a controllable electrochemical approach for large-scale synthesis of CDs with highly crystalline nature and excellent catalytic properties.[22] Bottom-up routes are also efficient methods to prepare CDs, including microwave treatment, hydrothermal synthesis, calcination methods, *etc.*

During these processes, CDs are formed from small molecules or oligomers. Accordingly, these methods offer exciting opportunities to control CDs towards a well-defined surface state, thus tuning their properties including emission wavelengths, quantum yield (QY) and so on.[20] For example, Ding *et al.* have proposed that nitrogen, sulfur co-doped CDs prepared from α-lipoic acid and ethylenediamine have a high QY, which is ascribed to the synergistic effect of nitrogen–sulfur groups from precursor molecules.[23]

### 2.3 Properties of CDs

Photoluminescence (PL), the most fundamental characteristic of CDs, is deeply influenced by synthetic routes and precursor resources (Fig. 3).[20] For example, bottom-up methods always result in CDs with a relatively higher QY, and specific precursors elicit a longer emission wavelength in the final CD products. Moreover, synthetic conditions should also be taken into account, such as the reaction temperature and quantity of reactive solvents. Besides QY and emission wavelength, broad PL profiles and excitation-dependent PL behaviors are also important features of CDs, which can be useful characteristics to understand the properties of CDs.

As energy storage materials, surface compositions and structures of CDs are of particular importance. For example, abundant groups and rich defects/edges on the surface of CDs play important roles in faradaic reactions, wettability between the electrode and electrolyte, oxygen electro-catalytic reactivity, *etc.*[24] More specifically, some surficial functional groups of CDs, like amino groups, make great contribution to the pseudocapacitance; carboxyl/hydroxyl groups help enhance the wettability between electrode materials and aqueous electrolytes;[25] and substantial defects/edges on the surface of CDs provide more exposure areas to make contact with oxygen molecules, which makes CDs efficient electrocatalysts.[26] Moreover, quantum sized CDs can also participate in the formation of metal oxide crystals. For example, CDs can coordinate with

some metal ions through their abundant surface functional groups, which bring about some significant impacts in the final products (composites of metal oxides/CDs), such as morphology and particle size.[27]

## 3. Next generation of electrochemical energy storage devices constructed from CDs

Supercapacitors, Li/Na/K-ion batteries, Li–S batteries, metal–air batteries and flow batteries will become an indispensable part of our life. From 3C electronics to electric motors and even electric power transmission, electrochemical energy storage devices play an important role in modern society.[28–31] For further development in future, more excellent new-generation batteries are highly desirable. Therefore, as the key part of energy storage devices, the performance of electrode materials is particularly important. CDs have their natural merits to construct better electrode materials, so as to solve many existing problems and bring about a significant development in supercapacitors and batteries.

### 3.1 Supercapacitors

High power density, high coulombic efficiency and long cycling-span are the features of supercapacitors.[32–35] Accordingly, supercapacitors play an important role in complementing or even replacing conventional batteries in the field of energy storage. Related applications of supercapacitors include load-leveling in solar or wind power, energy recovery in electronic vehicles, *etc.* However, compared to battery devices, low energy density and self-discharge are always the shortcomings of supercapacitors. To improve the electrochemical performance of supercapacitor electrodes, traditional carbon materials such as porous carbon, CNTs or emerging graphene-based materials are used to solve the above issues by enlarging the specific surface area, constructing porous structures, introducing pseudocapacitive reactions and improving electrical conductivity.[36–39] With the development of supercapacitors, some new perceptions have emerged gradually. For instance, only specific functional groups such as pyridine or pyrrole-type nitrogen could benefit the faradaic reactions, surface charge (including electrons and ions) transfer is crucial to the rate capability, micromorphology is also associated with the electrochemical performance, *etc.*[40–43]

Based on the above viewpoints, CDs can offer opportunities to construct capacitor electrodes with excellent performance. Taking electric double layer capacitors (EDLCs) as an example, Fan's group used highly crystallized GQDs to improve the overall conductivity, charge-transfer and ion migration kinetics of activated carbon.[44] In this process, GQDs could facilitate electrolyte ion transport and storage in deep and branched micropores (Fig. 4a, g and h). As a result, the GQD-embedded activated carbon possessed a microporous structure with a specific surface area of 2829 m$^2$ g$^{-1}$, achieving a remarkably high specific capacitance of 388 F g$^{-1}$ at 1 A g$^{-1}$ as well as excellent rate performance of over 60% retention at 100 A g$^{-1}$
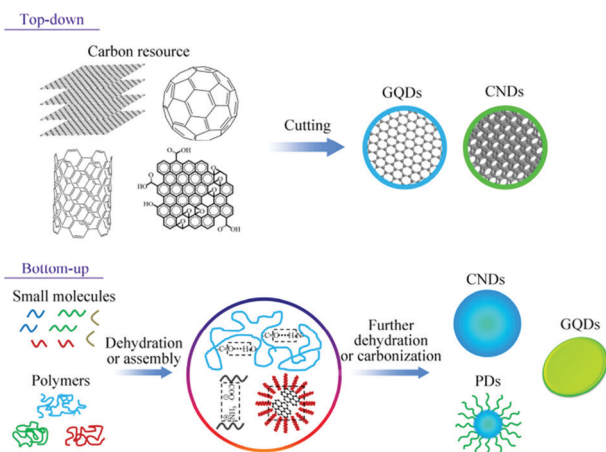
**Fig. 3** Main approaches to fabricate CDs: "top-down" cutting from different carbon-based materials and "bottom-up" synthesis from small organic molecules or polymers with low molecular weight. Reproduced with permission from ref. 20. Copyright 2015 Springer Nature.

**732** | *Mater. Chem. Front.*, 2020, **4**, 729–749

This journal is © The Royal Society of Chemistry and the Chinese Chemical Society 2020
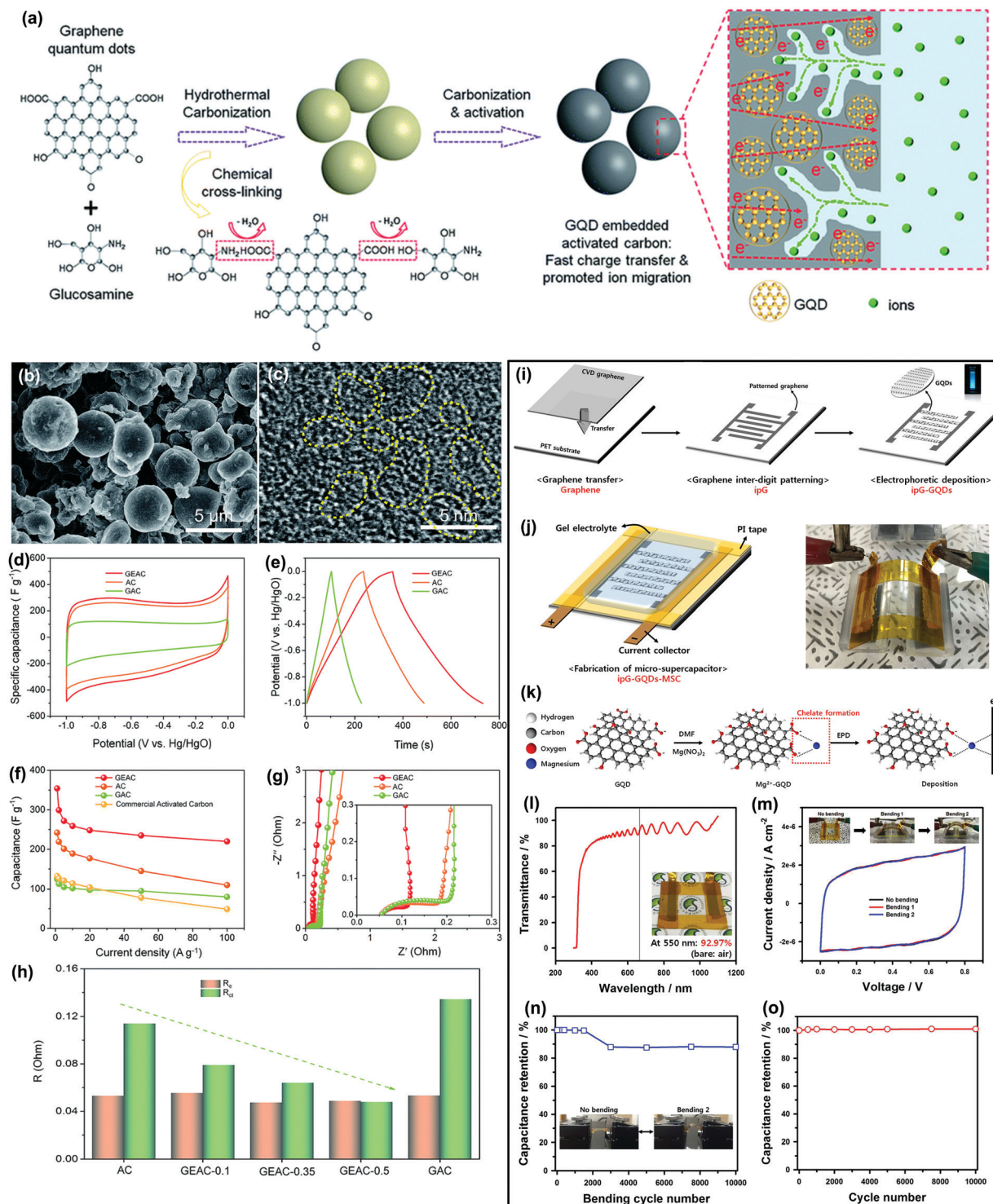
Fig. 4 (a) General preparation route of GQD embedded activated carbon (GEAC); the GEAC was prepared by hydrothermal carbonization of the GQD and glucosamine mixture, which was then pre-carbonized, and subsequently activated in a $N_2$ atmosphere. (b and c) SEM and TEM images of GEAC. Electrochemical performances in a three-electrode system: (d) CV curves at 10 mV s$^{-1}$; (e) charging/discharging curves at 1 A g$^{-1}$; (f) the rate performance plots; (g) the EIS plots; (h) the electrical resistance ($R_e$) and charge-transfer resistance ($R_{ct}$) of different samples. Reprinted with permission from ref. 44. Copyright 2019 Royal Society of Chemistry. (i) Schematic illustration for fabrication of an ipG-GQDs-MSC. (j) Optical image of a GQD MSC under bending. (k) Schematic illustration of the mechanism of the graphene–GQD electrophoretic deposition process. (l) UV spectra of the MSCs. (m) Cyclic voltammetry curves collected under various bending states. (n) Bending test from 180° to 45° for 10 000 cycles. (o) Cycling test at a scan rate of 10 V s$^{-1}$ for 10 000 cycles. Reprinted with permission from ref. 45. Copyright 2019 Royal Society of Chemistry.

(Fig. 4d–f). Besides this work, some other research teams also reported similar functions of CDs (especially GQDs) in EDLCs, such as improving the electrical conductivity, accelerating interfacial ion transport, enlarging the surface area, *etc.* Moreover, CD materials could also play an important role in transparent and flexible energy conversion and storage devices. Lee and his group reported a new concept to fabricate highly transparent and flexible micro-supercapacitors (MSCs) *via* a monolayer graphene and GQD chelate formed by a simple electrophoretic deposition method which combined graphene and GQDs to yield a graphene–GQD electrode (Fig. 4i–o).[45] With optical transmittance as high as 92.97%, the micro-device could exhibit a high capacitance of 9.09 $\mu$F cm$^{-2}$, capacitance retention of 100% over 10 000 cycles and a short relaxation time of 8.55 ms. Among the multiple factors related to the high performance, the rough surface and high conductivity generated by GQDs were especially crucial.

Recently, Xiong's group suggested a new method to improve negative electrodes (double-layer capacitance) in hybrid devices: building electron-rich regions by CDs on the surface of electrodes, so as to adsorb cations and accelerate the charge transfer at the same time (Fig. 5a).[11] According to the DFT simulation (charge distributions, Fig. 5d), some specific functional groups such as the phosphate group ($\sim$CPO$_3$), pyridine-type nitrogen or carboxyl could generate a significant change of charge in the surrounding atoms, while such influences from other functional groups including oxidized nitrogen or quaternary nitrogen were relatively limited. Through CDs, good carriers with properties such as controllable compositions,

adjustable surface groups, electron-rich regions were built on the surface of porous carbon. Such results were also supported by subsequent electrochemical tests. According to the results of cyclic voltammetry (CV), in alkaline, acidic and neutral electrolytes, the optimal capacitance of NPOCD/HPC (hierarchical porous carbon made from porous hydrogels and N, P, O doped CDs) was dramatically increased up to 40% over that of free-HPC (hierarchical porous carbon made from porous hydrogels as a blank sample). In particular, in neutral electrolytes without faradaic reactions, ion absorption mainly contributes to the capacitance. Therefore, electron-rich regions allow the carbon materials to absorb more cations. Such carbon materials, as novel negative electrodes (EDLC-type) for hybrid supercapacitors, have outstanding advantages in terms of energy density, and can also overcome the common shortcomings of carbon negative electrodes, such as self-discharge and mismatch with different positive electrode (pseudocapacitor-type or battery-type) materials.

Materials with pseudocapacitive behavior, such as some metal oxides (RuO$_2$, MnO$_2$) or polymers (polyaniline), can offer higher specific capacitance compared with electric double-layer capacitance type materials.[46–48] However, short life span and low rate capability are the main shortcomings of these materials. Accordingly, carbon material-incorporated composites have been proved to be effective materials to overcome these disadvantages, for instance, graphene–polymer composites, CNTs–metal oxide composites and so on. Compared to that, CD-based composites can go beyond this. Besides high surface area or good electrochemical conductivity, well dispersed CDs have better protection effect for polymer or metal oxide-based substrates. In terms of CDs–polymer composites, for example, Xie's group used a CDs–polyaniline hybrid as a supercapacitor electrode material by incorporating CDs into PANI fiber substrates, which had a good capacitance retention of 78.0% after 1000 charge–discharge cycles at a current density of 5.0 A g$^{-1}$.[49] An optimized result was achieved by Malik and his collaborators.[50] Novel fibrous GQDs–PANI composites showed an excellent specific capacitance of 1044 F g$^{-1}$ at a current density of 1 A g$^{-1}$ as well as a moderate cyclic stability retention of 80.1% after 3000 cycles. Beyond PANI, Liang's group developed a carbon quantum dot (CQD, belongs to CDs)-reinforced polypyrrole nanowire (PPy-NW), which was constructed *via* an electrostatic self-assembly strategy (Fig. 6a).[51] The electrochemical tests demonstrated that the as-made composite electrode had a high specific capacitance of 306 F g$^{-1}$ at a current density of 0.5 A g$^{-1}$ (Fig. 6d). The as-fabricated symmetric supercapacitor showed a high energy density (max) and power density (max), reaching 30.92 W h kg$^{-1}$ and 11.2 kW kg$^{-1}$, respectively (Fig. 6f). Moreover, good cycling capability with $\sim$85.2% capacitance retention after 5000 cycles also led to polypyrrole-based materials with a longer cycling life span. These results were attributed to CQDs which provided a larger surface area, more active edges and more conductive paths.

Metal oxides such as MnO$_2$ and RuO$_2$ are also promising pseudocapacitive materials with high theoretical specific capacitance (*e.g.*, 1370 F g$^{-1}$ of MnO$_2$). However, there are also some inevitable issues, such as unstable crystalline structure or
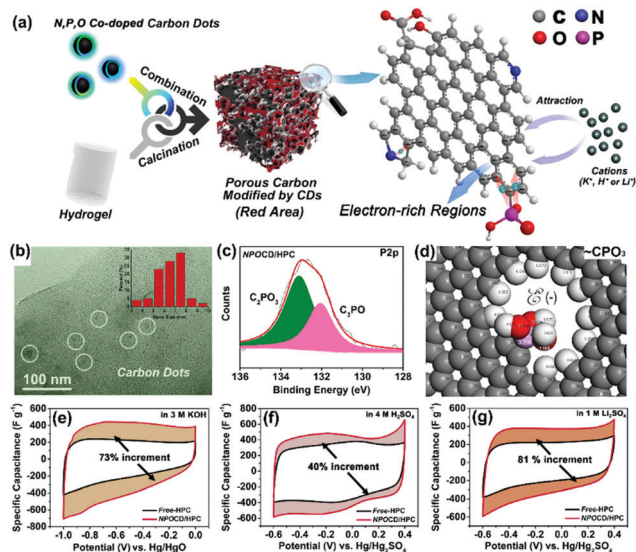


**Fig. 5** (a) Carbon dots and PAM hydrogels are the precursors of the porous carbon, which has abundant electron-rich defects for cation adsorption/reaction. For NPOCD/HPC, (b) TEM images and size distribution of carbon dots (inset image). (c) High-resolution XPS spectrum of P 2p. (d) DFT calculation results of the charge distributions of phosphorus ($\sim$CPO$_3$) groups and surrounding carbon atoms. CV curves of NPOCD/HPC and free-HPC (blank sample) at a scan rate of 10 mV s$^{-1}$ in (e) alkaline, (f) acidic, and (g) neutral aqueous solutions, respectively. Reproduced with permission from ref. 11. Copyright 2019, Wiley-VCH.

**734** | *Mater. Chem. Front.*, 2020, **4**, 729–749

This journal is © The Royal Society of Chemistry and the Chinese Chemical Society 2020
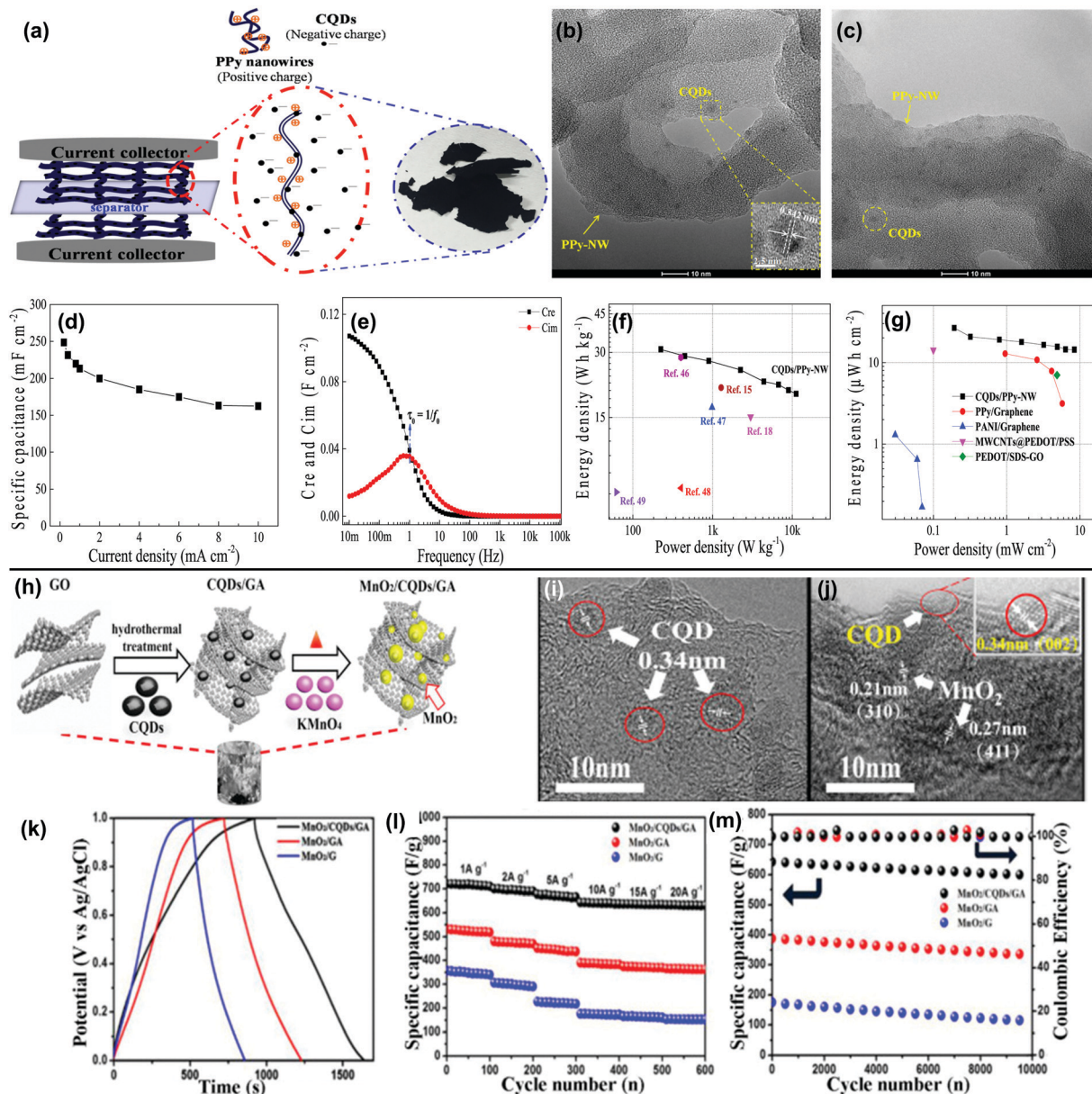
Fig. 6 (a) Scheme of electrostatic self-assembly synthesis of the CQDs/PPy nanocomposite. (b and c) Different magnification TEM images of CQDs/PPy nano wires. For the symmetric supercapacitor, (d) rate performance, (e) Bode plots of $C_{re}$ and $C_{im}$ of the specific capacitance versus frequency. Ragone plots of the device (f) based on the total mass of the active materials; (g) based on the geometric area of the supercapacitor. Reprinted with permission from ref. 51. Copyright 2017 Elsevier. (h) Scheme of the fabrication process of the $MnO_2$/CQDs/graphene composite aerogel. HRTEM images of (i) CQDs/GA and (j) $MnO_2$/CQDs/GA. (k) Charge−discharge curves (1 A $g^{-1}$), (l) rate performance, (m) cycling performances and coulombic efficiency of various samples. Reprinted with permission from ref. 52. Copyright 2018 Elsevier.

volume change effect, which affect the cycling life span and rate performance of the materials. Pioneering work was conducted by Ji et al.,[16] decorating $RuO_2$ with GQDs to obtain the composites. Surprisingly, such hybrids showed exceptional cycling stability with 96.9% capacity retention over 5000 cycles and those remarkable performances could be primarily ascribed to the significantly enhanced utilization of $RuO_2$ achieved by the efficient dispersion of GQDs and the formation of the GQD-based hybrid network structures, which could facilitate the fast charge transport and ionic motion during the charging–discharging process. The improvements stemmed from CDs also being applicable to

transition metal oxides. In the work conducted by Liu et al., CDs served as a bridge for connecting $MnO_2$ and graphene, which contributed to synthesizing a stable $MnO_2$–CDs–graphene composite aerogel.[52] Due to the connective function of CDs, stable combinations were formed between $MnO_2$ nanoparticles and graphene nanosheets. Subsequently, the as-fabricated composite aerogel exhibited a three-dimensional network structure, indicating a large specific surface area and abundant electron transport pathways. The optimal sample displayed a high specific capacitance of 721 F $g^{-1}$ at 1 A $g^{-1}$, good rate capability of 89.2% capacitance retention at 20 A $g^{-1}$ and a remarkable cycling stability of 92.3%

This journal is © The Royal Society of Chemistry and the Chinese Chemical Society 2020

Mater. Chem. Front., 2020, 4, 729–749 | 735

capacitance retention after 10 000 cycles at 10 A g$^{-1}$ (Fig. 6k–m). In brief, the advantages of the CD-pseudocapacitive material hybrids have shown a bright prospect for their better application in high-performance supercapacitors.

For battery-type electrodes in hybrid supercapacitors (HSCs), unsatisfactory electronic conductivities, the volume change effect and slow kinetics always lead to short life cycles.[53–55] The poor rate performances restrict the cycling life span and power density of HSCs. To overcome these shortcomings, graphene oxide, carbon nanotubes (CNTs), and active carbon have been employed to increase the surface area, surface wettability, and conductivity.[56–58] In fact, the incorporation of these carbon materials can only resolve the above problems partially, even causing some other side effects. For example, carbon with dense structures may hinder the contact between metal oxide particles and electrolytes. And too many carbon components will decrease the overall specific capacitance, because carbon materials provide a low contribution to capacitance. Meanwhile, there will be large improvement prospects for the composites when CDs are employed. First of all, CDs are more flexible for constructing desired structures than multi-dimensional carbon materials. Secondly, when CDs and metal oxides/hydroxides are assembled together, there will be numerous interspaces or pathways for both charge transfer and volume change. In addition, as mentioned above, CDs with small size and abundant defects/groups will benefit surface wettability, or full contact between composites and electrolytes for electrochemical reactions. Finally, good distribution of CDs will provide uniform surface states, which ensures the uniformity and stable cycling performances of final composite electrode materials. With assistance of CDs, NiCo$_2$O$_4$, Ni(OH)$_2$, NiCo$_2$S$_4$ and some other composites possess higher rate-capability and longer cycling life.[27,59,60]

A related investigation was conducted by Wei et al. to increase the graphitization degrees of CDs and employ them to prepare the CDs/NiCo$_2$O$_4$ nanocomposites.[27] Dramatically, multiple morphologies could be achieved for composites by changing the inventory rating of CDs in reactions, from sea urchin to flower and even bayberry (Fig. 7a–d). Correspondingly, microscopic structures of the composites were also changed for better rate performances. In comparison with nanoneedles (150 nm in diameter for an urchin like sample and 70 nm in diameter for a chestnut like sample), the nanopetals on a flower-like sample (ca. 30 nm in thickness) and the nanodots on a bayberry-like sample (ca. 30 nm in diameter) provided shortcuts to charge transfer (Fig. 7e), so that the latter two samples showed better rate performances. The optimal sample (flower like sample) exhibited a high specific capacitance of 2168 F g$^{-1}$ at a current density of 1 A g$^{-1}$. When the current density varied from 1 to 30 A g$^{-1}$, the retention rate of this sample reached 75.2% and it also exhibited exceptional cycling stability over 5000 cycles at different current densities, which was far beyond the performance of NiCo$_2$O$_4$ single crystals (NCO sample, Fig. 7f–i).

Applications of CDs in supercapacitors have fully shown their potential in constructing robust electrochemical capacitor devices. As for energy storage devices with more complex
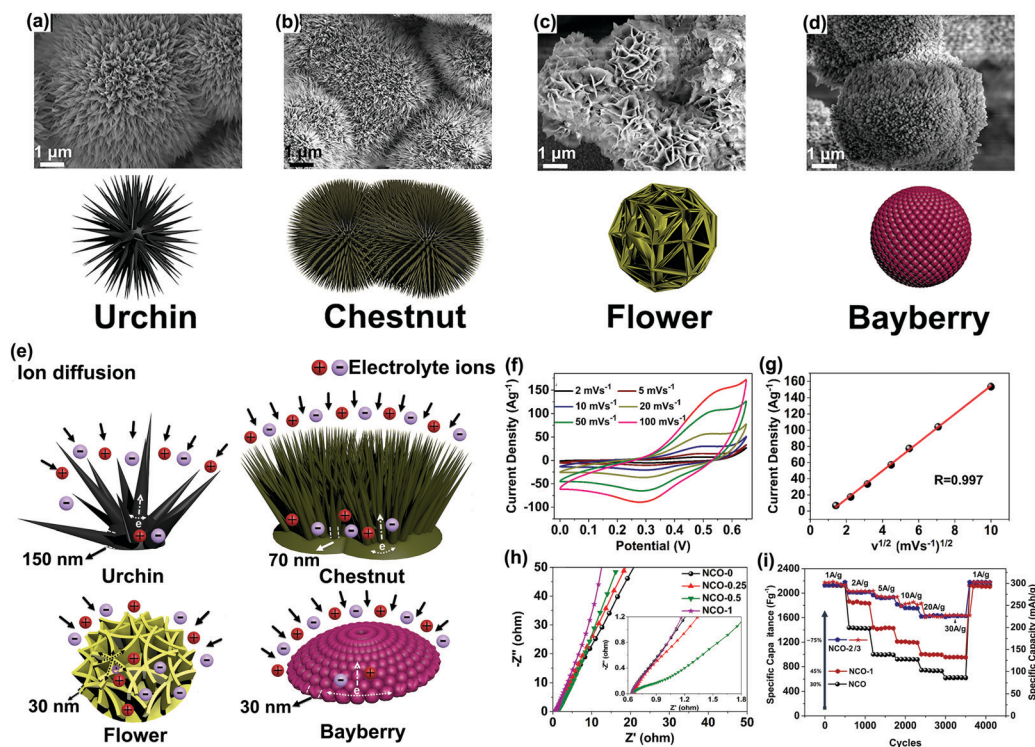


Fig. 7 (a−d) The CDs/NiCo$_2$O$_4$ composites with different morphologies. (e) Simulation of ion diffusion on the material surfaces. (f) CV curves and (g) the relationship between current density of the optimal sample (NCO-0.5). (h) Nyquist impedance plots at the open-circuit potential. (i) Cycling and rate performances at various current densities. Reproduced with permission from ref. 27. Copyright 2016, Wiley-VCH.

electrochemical reaction processes like battery systems, the mechanistic roles of CDs remain unclear and are worthy of explorations.

### 3.2 Lithium-ion batteries

Lithium ion batteries (LIBs) have been widely applied in many modern energy devices, such as wearable sensors, electric vehicles and portable electronic devices due to their stable electrochemical properties and high energy density.[61–63] Secondary LIBs are mainly composed of a cathode, an anode, a separator, electrolytes and an outer shell. Both electrodes act as $Li^+$ hosts with a separator membrane to avoid short circuit while the electrolyte supplies $Li^+$.[64] The specific capacity of electrode materials is a crucial factor to determine the specific energy of a battery. Lots of electronics, especially electrical vehicles, demand batteries with large energy densities. Therefore, exploring promising electrode materials has been considered as an important way to advance battery development.

First of all, we will introduce the working principle of LIBs. At the start of charging, Li ions are driven by the electrical potential supplied by an external power from the cathode into the electrolyte, and they diffuse toward anodes. Finally, Li ions are embedded in the anode, e.g., graphite, and form $Li_xC$, which is referred to as lithiation.[65] Meanwhile, electrons are transmitted into anodes through an external circuit; therefore, electricity is stored in the form of electrochemical energy. During the discharging process, Li ions are extracted from the anode and transferred back to the cathode because of the electrochemical potential difference between the anode and the cathode. According to conservation of charges, the anode loses electrons and the cathode gains them. The potential difference gradually decreases with the delithiation of the anode and eventually needs to be rebuilt. During the whole charging and discharging process, Li ions are repeatedly inserted/extracted between both electrodes, which is figuratively called "rocking chair batteries".

Carbon-based materials have been considered as one of the most promising candidates for electrode materials of LIBs, owing to their outstanding advantages, such as electrical conductivity, chemical stability and abundance resources.[66–68] At present, graphite anodes are commercialized due to low cost and high abundance. However, the theoretical specific energy of graphite is 372 mA h $g^{-1}$ (with $LiC_6$ final product), which leads to a limited specific energy.[69,70] For a higher energy density to cater for smaller devices, intensive efforts have been made in developing new anode materials such as metal-alloy-based materials (Si, Sn and P),[71–73] metal oxides,[74,75] Ti-based materials ($Li_4Ti_5O_{12}$, $TiO_2$),[76,77] and transition metal disulfides ($MoS_2$, $VS_2$).[78,79] All materials mentioned above require different strategies to improve their respective inherent defects. CD coating is an effective strategy to solve many issues, for example, improving electrical and ionic conductivity, increasing the specific surface area of composite materials and enhancing the lithium storage capacity.

Transition metal oxides could be considered as high capacity candidates for anode materials through a conversion reaction mechanism ($MO_x + 2x\text{Li} \leftrightarrow \text{M} + x\text{Li}_2\text{O}$), including FeO, $Fe_3O_4$, NiO, $Co_3O_4$, $Mn_3O_4$ and CuO.[80–84] However, the low electrical conductivity and volumetric expansion of transition metal oxides is a main problem for commercialization. Ji's research group designed a C quantum dot-coated $Mn_3O_4$ composite ($Mn_3O_4$/Cdots) via a green alternating voltage electrochemical approach (Fig. 8a).[81] It is worth noting that the introduction of C quantum dots could induce the morphology of $Mn_3O_4$ particles to form an octahedral structure. The $Mn_3O_4$/CDs composite demonstrated great electrochemical performances, exhibiting an improved reversible capacity of 934 mA h $g^{-1}$ after 50 cycles at 100 mA $g^{-1}$, which was almost five times as much as that of pure $Mn_3O_4$. Then, a self-supporting and binder-free coal-based graphene quantum dot and $\alpha$-$Fe_2O_3$ (C-GQDs/$\alpha$-$Fe_2O_3$) composite electrode was fabricated by Qiu et al. (Fig. 8b).[85] The composite electrode eliminated the use of an additional binder, which could increase the ion transfer, electrical conductivity and specific capacity. The capacity of the C-GQDs/$\alpha$-$Fe_2O_3$ composite was up to 1582.5 mA h $g^{-1}$ at 1 A $g^{-1}$, and it maintained 1320 mA h $g^{-1}$ after 110 cycles. The capacity was still maintained at 1091 mA h $g^{-1}$ at a high current density (5 A $g^{-1}$). In addition, the initial Coulombic efficiency reached up to 78.04%. Fan et al. have designed and successfully synthesized CuO + Cu + GQD (CCG) triaxial nanowire arrays for performance improvement as an LIB anode (Fig. 8c and d).[84] It was the first time that GQDs were applied in surface engineering of LIB electrodes. The CCG anode delivered a high rate capability and excellent long-term cyclability. Furthermore, the initial coulombic efficiency (87%) was significantly improved, which could be attributed to the synergetic contribution from the Cu and GQD layers. Moreover, binary transition metal oxides as a type of anode material for LIBs have been widely explored due to their good electrochemical activity, more redox reactions and the remarkable synergistic effect between two different metal species. Wang et al. designed Co–Ni bimetal oxide spheres via a one-step solvothermal method. The composite material had richer metal valence variations and higher electrical conductivity than $Co_3O_4$ or NiO.[82] NiO@$Co_3O_4$ hollow spheres decorated with graphene quantum dots (NiO@$Co_3O_4$@GQDs) were synthesized, which obviously reduced the interphase resistance and increased the surface area for electrochemical reactions because of adding GQDs. It could deliver a large reversible capacity of ~1327 mA h $g^{-1}$ after 250 cycles at 0.1 A $g^{-1}$.

Ti-Based materials have attracted a high level of scientific attention as an advanced lithium storage system given their outstanding high-rate capacity and cycling stability, improved safety and negligible volume expansion.[86–88] However, their vital drawbacks are low electronic conductivity and ion diffusion coefficient, which lead to severe polarization during cycling. Spinel $Li_4Ti_5O_{12}$ (LTO) is very competitive among commercial materials for LIBs. As shown in Fig. 9a, Kim et al. successfully fabricated novel LTO/nitrogen and sulfur co-doped graphene quantum dots (LTO/N,S-GQDs).[89] The introduction of N,S-GQDs not only increased both ultrafast electron transfer and electrolyte transport but also enhanced the specific capacity. The specific discharge capacity was 254.2 mA h $g^{-1}$ at 0.1C and 126.5 mA h $g^{-1}$

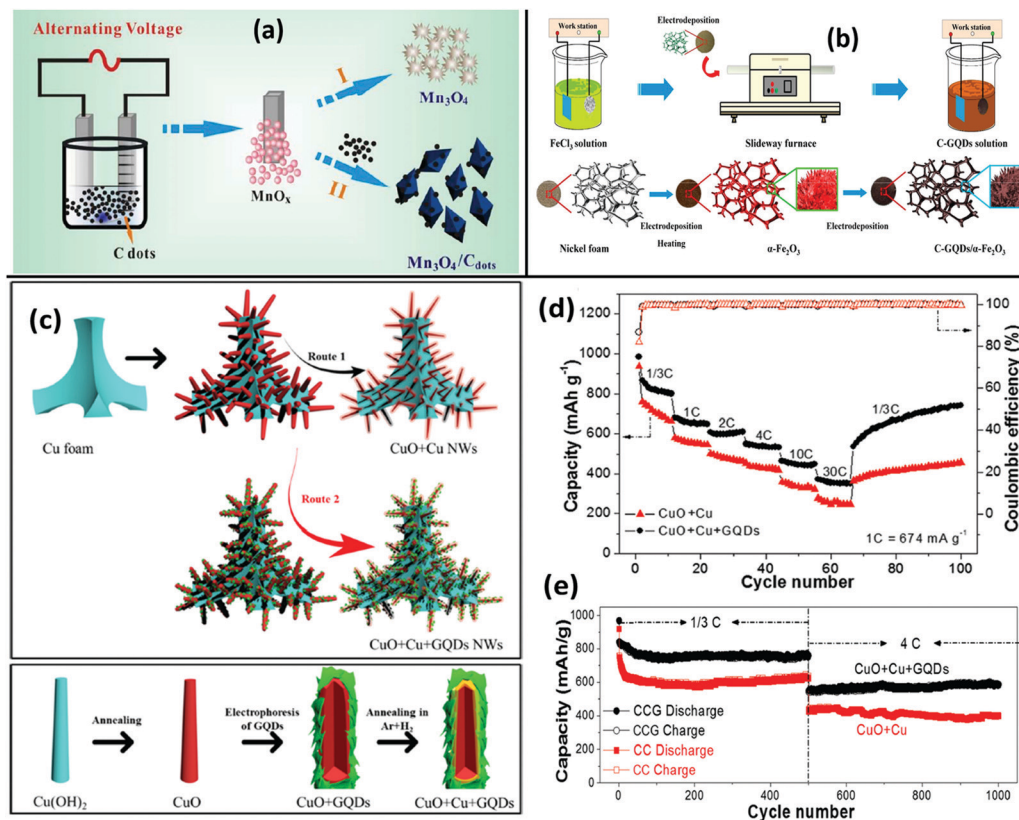This journal is © The Royal Society of Chemistry and the Chinese Chemical Society 2020

*Mater. Chem. Front.*, 2020, **4**, 729–749 | **737**

**Fig. 8** (a) Schematic representation of $Mn_3O_4$ and $Mn_3O_4$/Cdots composite. Reprinted with permission from ref. 81. Copyright 2015, Royal Society of Chemistry. (b) Preparation of C-GQDs/$\alpha$-$Fe_2O_3$ composites. Reprinted with permission from ref. 85. Copyright 2019, Elsevier. (c) Schematic of the fabrication process of CuO-based nanowire electrodes. Route 1 is for CuO + Cu (CC) core/shell nanowires. Route 2 is for CuO + Cu + GQD (CCG) triaxial nanowires; electrochemical characterization of CCG and CC anodes; (d) rate performance with coulombic efficiency; (e) cycling performance at 1/3C for the first 500 cycles and 4C for the second 500 cycles. Reprinted with permission from ref. 84. Copyright 2014, Wiley-VCH.

at 10C. The capacity remained at 96.9% at least after 2000 cycles at 2C. Similarly, Liu's research group proposed a simple method for coating LTO with an ultrathin protective and charge-transport layer of N-functionalized graphene quantum dots (N-GQDs) through a solution-based process (Fig. 9b).[90] LTO-NGQDs displayed remarkable electrochemical performances, including cycling stability (171 mA h $g^{-1}$, 200 cycles at 20C) and rate capability (0.2–50C). The role of GQDs as an interfacial layer is as a charge transfer layer that protects the $Li_4Ti_5O_{12}$ electrode from reactions with the electrolyte. Banks *et al.* combined the advantages of carbon dots, doping and structural design to synthesize an N-$TiO_2$/C-dots composite material for LIBs.[91] It can deliver a capacity of 185 mA h $g^{-1}$ with 91.6% retention even at a high rate of 10C over 1000 cycles. Apparently, compared with pure $TiO_2$, the addition of carbon dots significantly improves the electrical conductivity and charge transfer reactions.

$MoS_2$, which belongs to transition metal disulfides, is receiving intensive research interest for LIBs because of its unique physical and chemical properties. However, a pure $MoS_2$ anode is hampered by its intrinsic pulverization during $Li^+$ insertion/extraction, which leads to rapid capacity fading and poor cycle performance.[78] Nevertheless, the doping of GQDs could give $MoS_2$ advantages in structure and composition. Doong *et al.* fabricated boron-doped graphene quantum structure/$MoS_2$

(BGQS/$MoS_2$) composite materials as shown in Fig. 9c.[92] The boron-doped graphene quantum structure possessed the advantages of both 0-D graphene quantum dots and 2-D reduced graphene oxide. The BGQS/$MoS_2$ nanohybrid displayed superior rate capability and a highly reversible capacity. In addition, the reversible capacity remained at 1041 mA h $g^{-1}$ at 100 mA $g^{-1}$ after 50 cycles. After modification with GQDs, $MoS_2$ obviously boosted the electrochemical performance, improved the electrical conductivity and buffered volume change during the charging/discharging process.

There are a lot of problems to be solved in traditional electrode materials. The low electrical conductivity and volumetric expansion of transition metal oxides are the vital problem for commercialization. Similarly, the main drawbacks of Ti-based materials are low electronic conductivity and ion diffusion coefficient. Transition metal disulfide anodes are also hampered by their intrinsic pulverization during $Li^+$ insertion/extraction, which leads to rapid capacity fading and poor cycle performance. The introduction of CDs is an effective strategy to solve many issues from various aspects. CDs significantly enhance the electrical conductivity and charge transfer reactions. In addition, CDs with a large specific surface area could be conducive to the contact between the electrode materials and the electrolyte. What's more, the unique quantum size effects and rich surface

**738** | *Mater. Chem. Front.*, 2020, **4**, 729–749

This journal is © The Royal Society of Chemistry and the Chinese Chemical Society 2020
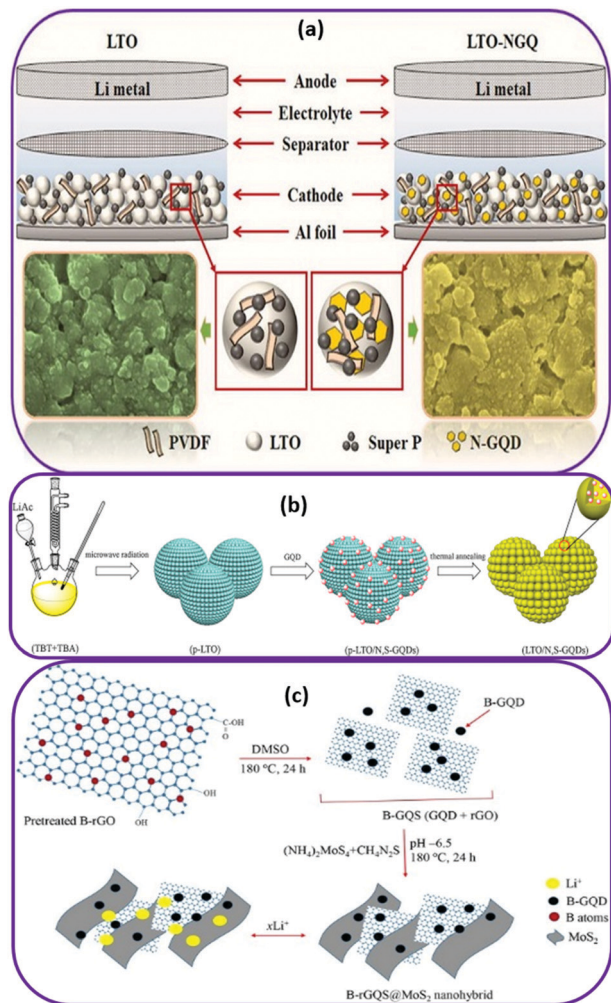
Fig. 9 (a) Schematic of LTO/NGQD and pristine LTO as anode materials. Reprinted with permission from ref. 89. Copyright 2019, Elsevier. (b) Procedure for the synthesis of LTO/N,S-GQDs. Reprinted with permission from ref. 90. Copyright 2015, Elsevier. (c) Schematic illustration of preparation of BGQS/MoS$_2$ nanohybrids and the application for Li$^+$ ion intercalation/deintercalation. Reprinted with permission from ref. 92. Copyright 2019, Frontiers.

functional groups endow CDs with a dominating role in enhancing the structure stability and sustainability so as to buffer volumetric expansion during Li$^+$ insertion/extraction.

### 3.3 Sodium-ion batteries

In recent years, with the increasing demand for low cost, long lifetime, high energy density storage systems, an extensive amount of effort has recently been devoted to the development of sodium-ion batteries (SIBs).[93–95] SIBs have been recognized as a promising substitute to LIBs owing to the abundant supply and low cost of sodium. However, due to the large Na$^+$ ion radius (55% larger than Li$^+$ ions), the application of already well-developed electrode materials for LIBs in SIBs is always inefficient.[96,97] For example, graphite has been commercialized in LIBs, but it is not applicable in SIBs due to its small interlayer spacing. Silicon has been highlighted as a promising

anode material because of its superior specific capacity and small volume changes.[98] Nevertheless, it is difficult to form sodium–silicon alloys, which makes it unsuitable for electrode materials of SIBs. Therefore, exploration of commercial and practical anode materials for SIBs is a pressing need at present. Nowadays, carbon materials are the anode materials with large potential for commercialization, including hard carbon, graphene, doped carbon and carbon dots.[99–102]

In fact, sodium-ion full cells were assembled using hard carbon as the anode. However, it has to be considered that the initial coulombic efficiency of hard carbon anodes is generally low. Many researchers adopted presodiation and desodiation to solve that problem, which, however, is costly and hard to commercialize. In fact, CDs often play a critical role in improving the first coulombic efficiency and electro-chemical performance in LIBs, as they do in SIBs. Moreover, CDs, known as "design additives", can regulate the structure and morphology of electrode materials to enhance the electro-chemical performance and the initial coulombic efficiency. CDs as raw reaction products could transform into frameworks composed of nanosheets under rapidly increasing temperature with the catalysis effect of Na. Then, the as-yielded nanosheets displayed a cross-linked 3D framework structure through the combination with multitudinous O-rich functional groups. Ji and co-workers firstly applied 3D porous carbon frameworks (PCFs) as anode materials for SIBs which exhibited a superb electrochemical performance (5 A g$^{-1}$, 99.8 mA h g$^{-1}$, 10 000 cycles, Fig. 10a).[102] Fan's group synthesized edge-nitrogen-rich CD-pillared graphene blocks (N-CDGBs) for SIBs with excellent rate capacity, ultrahigh volumetric/gravimetric capacity and ultralong-term cycling stability, as shown in Fig. 10b.[103] The strategy for the synthesis of N-CDGBs was that an aniline monomer was self-polymerized into graphene oxide blocks, and subsequently carbonized. Owing to the high bulk density, high content of edge-nitrogen (95%), and large edge-interlayer spacing, the N-CDGBs as an anode delivered a capacity of 520 mA h g$^{-1}$ at 0.02 A g$^{-1}$. Moreover, the densely pillared structure of N-CDGBs with robust structural stability, more active sites, overall conductive network, and fast ion transfer channels could be well maintained after 10 000 cycles at 10 A g$^{-1}$. From what has been discussed above, CDs play a determining role in structural design. Recently, Javed *et al.* directly used individual CDs as anode materials for SIBs, as shown in Fig. 10c,[104] which demonstrated a superior and stable rate performance. At the end of the rate performance when the current density was reverted to the original 0.5C, the CD electrode was still capable of presenting 350.9 mA h g$^{-1}$ and a capacity retention of 72.4% after 500 charge/discharge cycles.

Ti-Based materials are also regarded as an alternative anode material owing to their negligible volume expansion with a reasonable working potential. However, the poor electronic and ion conductivities remain a major obstacle for their practical applications.[105–107] In recent years, more and more research teams chose to combine Ti-based materials and CDs to solve those problems. Banks and co-workers fabricated SIBs using N-doped TiO$_2$ nanorods decorated with carbon dots (N-TiO$_2$/C-dots)

This journal is © The Royal Society of Chemistry and the Chinese Chemical Society 2020

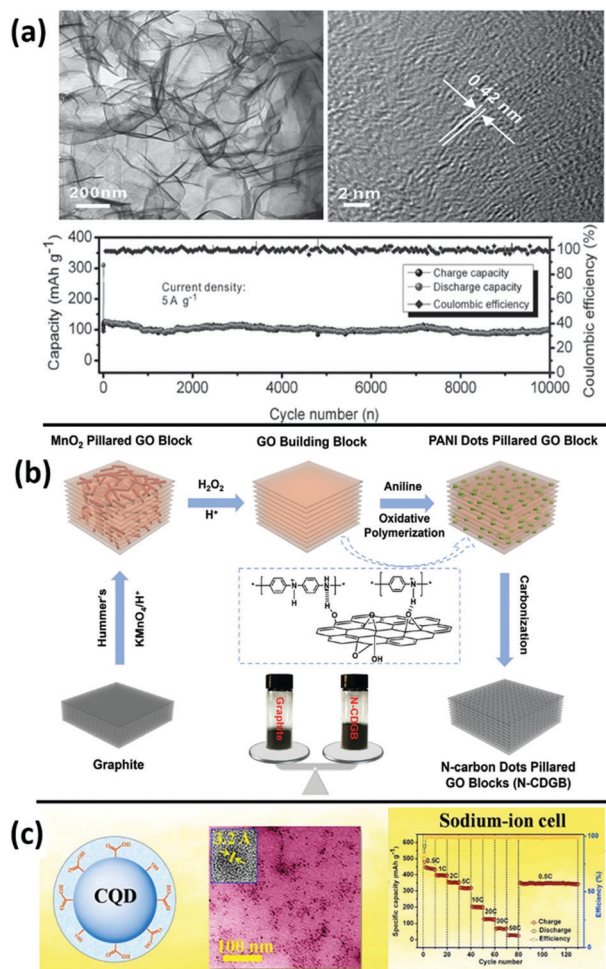*Mater. Chem. Front.*, 2020, **4**, 729–749 | **739**

Fig. 10 (a) TEM and HRTEM images of CD-derived 3D porous carbon frameworks (PCFs); cycle performance of PCFs as an anode for sodium ion batteries; reprinted with permission from ref. 102. Copyright 2015, Wiley-VCH. (b) Schematic illustration of the fabrication process for N-carbon dot pillared GO blocks (N-CDGB). The weight of the corresponding samples is 150 mg; reprinted with permission from ref. 103. Copyright 2018, Wiley-VCH. (c) The schematic illustration and TEM of CDs; rate performance and corresponding CEs of the CD electrode at 0.5–50C. Reprinted with permission from ref. 104. Copyright 2018, Elsevier.

composite anode materials (Fig. 11a).[91] The N-TiO$_2$/C-dots anode materials exhibited improved electrical conductivity and charge transfer performances owing to the decorating C-dots, N-doping, and nanostructure design. More importantly, as displayed in Fig. 11b, the first coulombic efficiency of the N-TiO$_2$/C-dots composite electrode was 41.6%, which was more than twice the value reported for TiO$_2$. Meanwhile, the specific capacity of the N-TiO$_2$/C-dots composite could reach 166 mA h g$^{-1}$ with 93.6% retention at 5C after 300 cycles. The obtained N-TiO$_2$/C-dots displayed excellent cyclic stability and superior rate capability. Then the research group of Ji used CDs as an additive to produce graphene-rich petal-like rutile TiO$_2$ (G/P-RTiO$_2$).[108] The petal-like structure consisting of nanoneedles is beneficial to shorten the transport path of sodium ions. As a result, G/P-RTiO$_2$ as an anode in SIBs delivered a high capacity of 245.3 mA h g$^{-1}$ at 0.25C and good initial coulombic efficiency

of about 50.6%. Strikingly, G/P-RTiO$_2$ still maintained a specific capacity of 74.6 mA h g$^{-1}$ with a retention of 94.4% at an extremely high rate of 10C after 4000 cycles. Yang *et al.* designed a novel binder-free anode using N-doped graphene quantum dots (N-GQDs)-decorated Na$_2$Ti$_3$O$_7$ nanofiber arrays (Na$_2$Ti$_3$O$_7$ NFAs) directly grown on flexible carbon textiles (CTs) for SIBs (Fig. 11c and d).[109] It delivered a capacity of 306 mA h g$^{-1}$ at 0.5C, superior rate capability and good capacity retention ($\sim$92.5% after 1000 cycles at 4C). More importantly, the soft protection provided by the novel N-GQDs resulted in greatly increased surface conductivity and stability of the nanofiber array structure, leading to high Na-ion diffusion kinetics.

Due to the excellent properties of CDs, they have also been used as cathode materials for SIBs. Vanadium dioxide (VO$_2$) has been long regarded as a promising electrode material for LIBs and SIBs owing to its high capacity, low cost, and abundant sources.[17,110,111] However, VO$_2$ as an electrode material suffers from fast capacity fading and poor rate performance due to self-aggregation, dissolution, and the rapidly increasing charge transfer resistance during cycles. Therefore, surface engineering by coating graphene quantum dots (GQDs) can secure high surface conductivity and sustain the structure integrity of VO$_2$. Fan and co-workers demonstrated that coating VO$_2$ array with an additional GQD layer brought further advantages in enhancing the electrochemical performance in SIBs.[17] It showed a high capacity of 306 mA h g$^{-1}$ and superior rate tolerance and good capacity retention (88% after 1500 cycles at 18 A g$^{-1}$). Tong's group also designed a new-type of free-standing CQD-coated VO$_2$ interwoven nanowire by a simple fabrication process. The CQD nano-surface-engineered VO$_2$ electrode exhibited a capacity of 328 mA h g$^{-1}$ at a current density rate of 0.3C for sodium storage. The CQDs that are highly flexible for surface engineering served the function of protecting the nanowire surface and played an important role in the diffusion of electrons.

In various electrode materials of SIBs, such as Ti-based materials, V-based materials and two-dimensional transition metal sulfides, the emergence of CDs brought many miraculous effects. Firstly, CDs, like other carbon-based materials, could work as conductive materials to enhance the ion/electron transfer and provide a larger surface area with richer active sites to boost electrochemical performance. Secondly, the unique advantage of CDs is that they could enhance the initial coulombic efficiency and facilitate full contact between the electrode materials and the electrolyte due to surface wettability. Thirdly, in comparison, the addition of only a small quantity of CDs can achieve the same effect as other carbon materials. Therefore, CDs could maintain as large energy densities as possible for SIBs. In a nutshell, the decoration of CDs is a new approach to boost the performance of SIBs in all respects.

### 3.4 Potassium-ion batteries

To date, potassium-ion batteries (PIBs) have been a promising alternative to LIBs because potassium is an abundant natural resource and is cost-effective.[112,113] PIBs share similar working principles with LIBs and SIBs, called "rocking chair" rechargeable batteries. However, the electrode materials are still in the early stage of exploration.
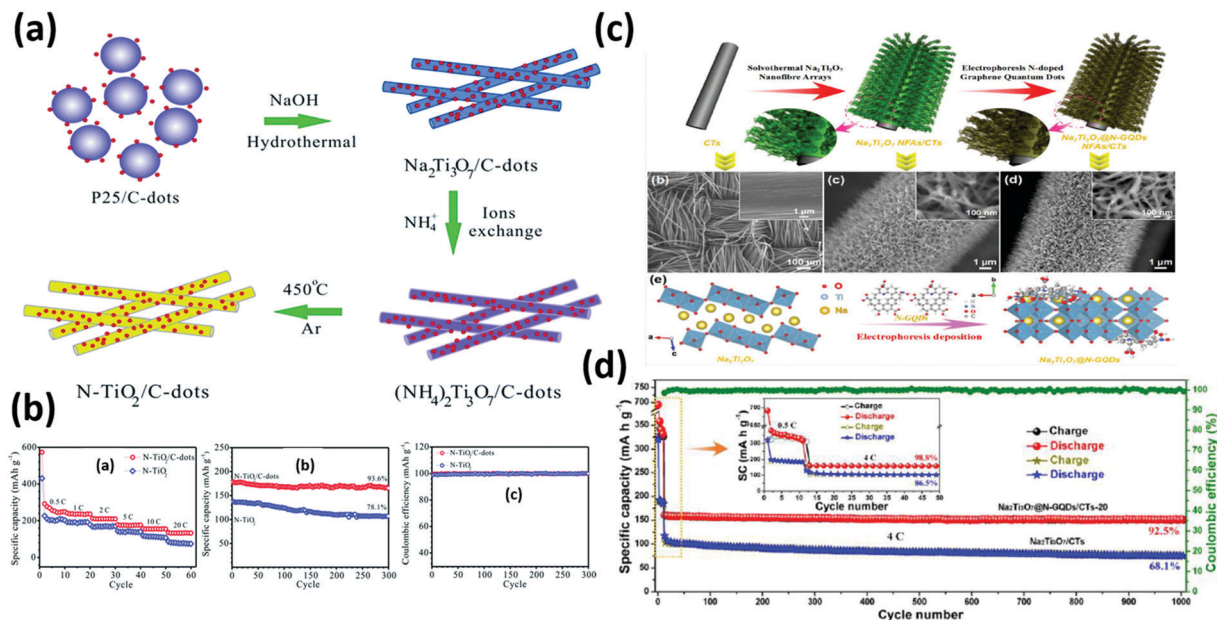
**740** | *Mater. Chem. Front.*, 2020, **4**, 729–749

This journal is © The Royal Society of Chemistry and the Chinese Chemical Society 2020

**Fig. 11** (a) Illustration of the fabrication process to produce N-TiO$_2$/C-dot composites; (b) galvanostatic discharge/charge voltage profiles at different rates of SIBs employing the N-TiO$_2$ and N-TiO$_2$/C-dot anodes. (b-a) Rate capability, (b-b) cycling performance at 5C and (b-c) coulombic efficiency of sodium-ion batteries employing the N-TiO$_2$ and N-TiO$_2$/C-dot anodes; reprinted with permission from ref. 91. Copyright 2015, Royal Society of Chemistry. (c) (c-a) A schematic illustration of the preparation of Na$_2$Ti$_3$O$_7$@N-GQDs NFAs on flexible carbon textiles. (c-b–c-d) The corresponding SEM images. (c-e) Geometrical models of both the Na$_2$Ti$_3$O$_7$ NFAs and Na$_2$Ti$_3$O$_7$@N-GQDs NFAs; (d) long-term cycling performances of Na$_2$Ti$_3$O$_7$@N-GQDs/CTs and Na$_2$Ti$_3$O$_7$/CTs electrodes at different current densities of 0.5C and 4C, respectively. Reprinted with permission from ref. 109. Copyright 2019, Royal Society of Chemistry.

Carbon materials are still one of the hot candidates for PIB anodes, such as graphite, reduced graphene oxide, hard carbon, soft carbon, and few layered graphene.[114–118] Hard carbon has a more disordered nanostructure, creating more space to buffer the dramatic volume change. In addition, HC usually could deliver capacities above 0.1 V, which is higher than the plate potential of potassium, reducing the risk of dendrite formation. Ji et al.[119] obtained honeycomb-like hard carbon (HHC) as an anode material from carbon quantum dots (CQDs) as shown in Fig. 12. The CQDs as raw materials play a crucial role in the structure of HHC. Due to its unique characteristics, HHC demonstrated a high reversible specific capacity of 195.3 mA h g$^{-1}$ at 0.1 A g$^{-1}$ and 67.43% capacity retention after 150 cycles.

The research of PIBs is still in its infancy. Traditional electrode materials with a CD coating or a composite are not explored extensively. Nevertheless, CDs are the key factor to construct various nanostructured carbons as anode materials. The hollow or honeycomb interior and tiny tunnels formed by the pyrolysis of CDs were beneficial for the infiltration of electrolyte and diffusion of K$^+$, leading to the improvement of electrochemical properties. In addition, the incorporation of nitrogen caused the generation of numerous exposed surface defects, which were favorable for potassium storage. Overall, the neoteric template action of CDs provided informative and prospective guidance for the design of electrode materials.

### 3.5 Lithium–sulfur batteries

Lithium–sulfur (Li–S) batteries have attracted increasing attention in overcoming the limitations of current energy storage
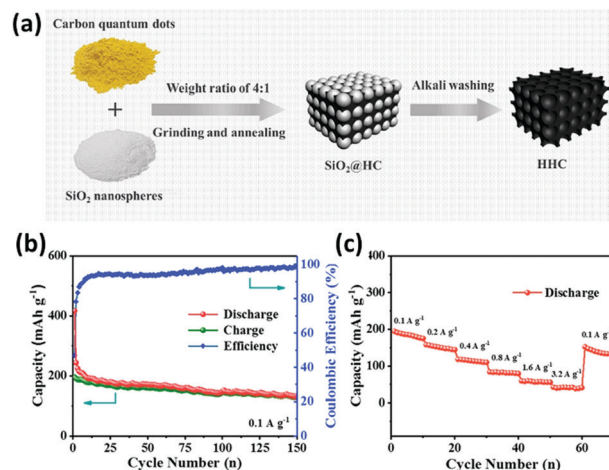


**Fig. 12** (a) The designed illustration of honeycomb-like hard carbon (HHC); (b) cycling performance at 0.1 A g$^{-1}$; (c) rate capability at various current densities. Reprinted with permission from ref. 119. Copyright 2019, Elsevier.

devices by delivering high specific energy and excellent cyclic stability. However, Li–S batteries have several technical barriers such as low electrical and ionic conductivities of sulfur, high volume change upon lithiation, irreversible loss of polysulfide anions due to dissolution in the electrolyte, sulfur shuttling between the anode and cathode, and decreasing number of electrochemically active reaction sites during battery operation.[120–123] All these limitations restrain the commercial progress of Li–S batteries. To solve the above-mentioned issues, all kinds of

carbon materials, such as graphene, carbon nanotubes, porous carbon, and carbon dots,[124–126] have been integrated with the sulfur cathode matrix and the modified separator because of their outstanding physicochemical properties to maximize the utilization of sulfur and restrain the dissolution of polysulfides.

Among all these carbon materials, carbon dots, known for their excellent photoluminescence properties, are enriched with oxygen functional groups on their edges. In addition, carbon dots could evenly cover the target materials owing to their small size. Actually, carbon dots have been reported to serve as cathode composite materials to yield high performance Li–S batteries. Park and co-workers firstly integrated a graphene quantum dots (GQDs)–sulfur composite cathode in Li–S batteries (Fig. 13).[127] GQDs were obtained by a modified Hummers' process. GQD–S/carbon black (CB) were then fabricated by a simple hydrothermal method. After 20 cycles in the charged state, GQDs tightly coated the surface of the nanosized sulfur particles, which was confirmed by lattice fringes corresponding to the (111) planes. C–S bonding that originated from the oxygen-rich functional groups at the edge of the GQDs was confirmed by DFT calculation and XPS. In addition, the discharge profiles illustrated that $Li_2S$ was prepared after the reduction of $S_8$, which resulted in a theoretical capacity of 1675 mA h $g^{-1}$. The GQDs-S/CB showed

better rate capability, better cyclability and higher coulombic efficiency than S/CB.

In order to meet the requirements for commercialization of Li–S batteries, high-area sulfur loading and current density have become the critical factors. Xiong et al.[128] successfully prepared polyethylenimine-functionalized carbon dots (PEI-CDots), which showed high area capacity at high current densities ($>8$ mA $cm^{-2}$). Subsequently, PEI-CDots@AB/S cathode materials were prepared by casting a mixture of PEI-CDots, acetylene black (AB), sulfur and polyvinylidene difluoride (PVDF) onto an Al foil current collector (Fig. 14). During the discharge process, sulfur is reduced to soluble polysulfide (LiPS) species. Then, the soluble LiPSs are further reduced to insoluble $Li_2S$ on the surface of the PEI-CDot-modified AB. As shown in the galvanostatic charge–discharge profiles, PEI-Cdots @AB/S well preserved the multi-step reaction plateaus under high current densities of up to 10 mA $cm^{-2}$, suggesting the more improved interfacial kinetics than that of AB/S. Meanwhile, the high-loading PEI-CDots@AB/S cathode exhibited excellent electrochemical properties at a current density of 8 mA $cm^{-2}$, which offered an area capacity of 3.3 mA $cm^{-2}$ over 400 cycles. In addition, modification of the separator by CQDs could also provide a physical shield against polysulfide shuttling and chemical adsorption of polysulfides. Xia's group first designed an ultralight multiwalled carbon nanotube/N-doped carbon
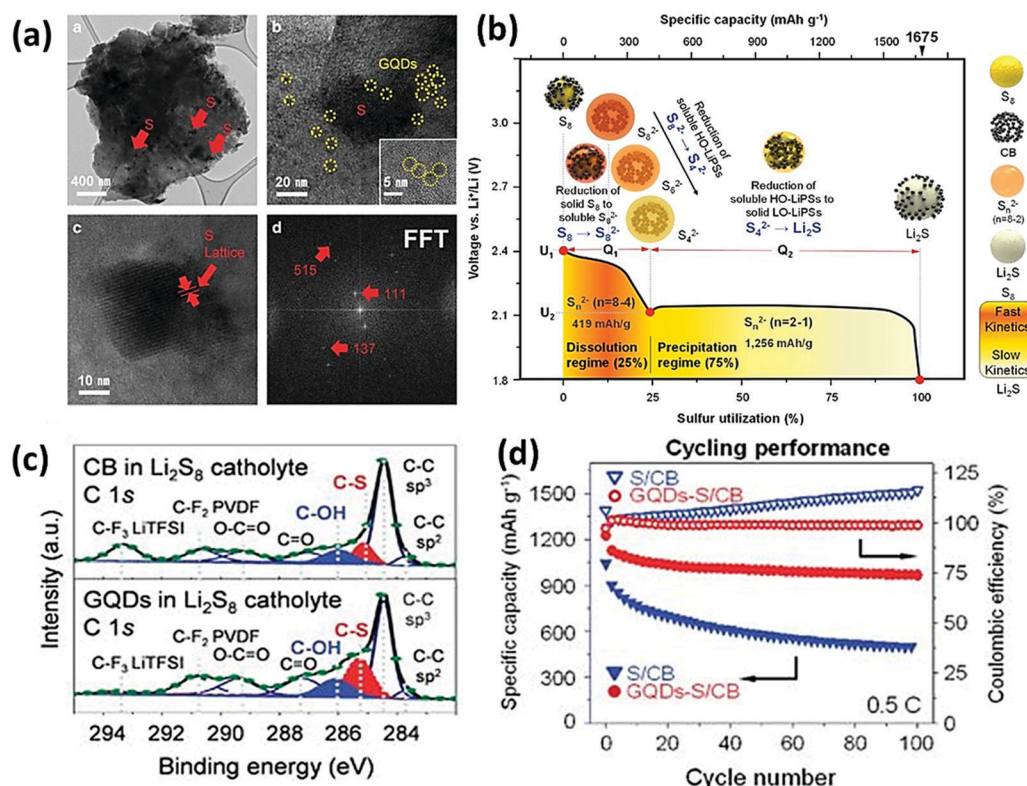


Fig. 13 (a) TEM and scanning TEM images of nanosized sulfur on GQD electrodes in $Li_2S_8$ catholyte after 20 cycles in the charged state. (b) Schematic illustration of the discharge profile of a conventional Li–S battery. HOPSs ($S_n^{2-}$, $n = 8$–4) and low-order polysulfides ($S_n^{2-}$, $n = 2$–1) are abbreviated as HO-PSs and LO-PSs, respectively. The onset potential ($U$) and the capacity ($Q$) in the dissolution and precipitation regimes are noted, which facilitates the analysis of the electrochemical properties of each sample. (c) C 1s high-resolution XPS spectral analysis of GQDs and the CB electrode in $Li_2S_8$ catholyte. (d) The cycling performance and coulombic efficiency at 0.5C over 100 cycles. Reprinted with permission from ref. 127. Copyright 2016, NPG Asia Materials.
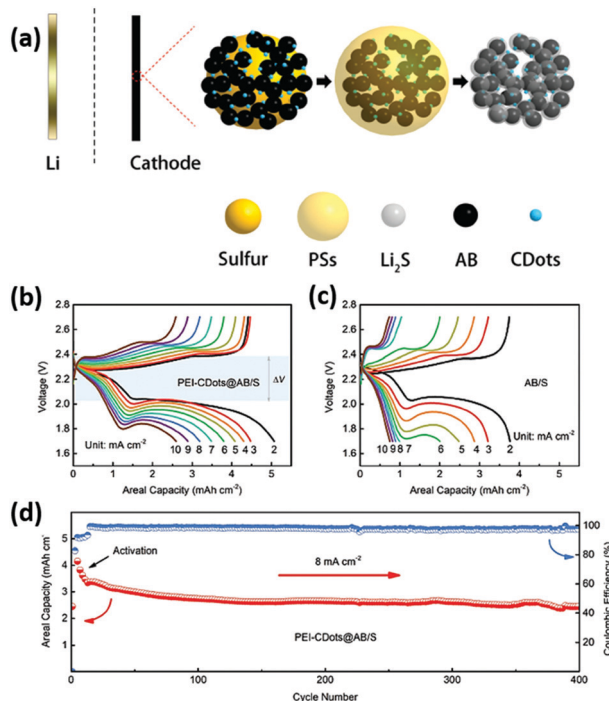
**742** | *Mater. Chem. Front.*, 2020, **4**, 729–749

This journal is © The Royal Society of Chemistry and the Chinese Chemical Society 2020

**Fig. 14** (a) Illustrations of the PEI-CDots-modified cathode composite at different charge−discharge stages. The charge/discharge profiles of (b) the PEI-CDots@AB/S cathode and (c) the AB/S cathode between 1.7 and 2.7 V. (d) The long-term cycling performance of the PEI-CDots@AB/S cathode with a sulfur loading of 6.6 mg, activated from 2 to 8 mA cm$^{-2}$ with 1 mA cm$^{-2}$ interval between each cycle. Reprinted with permission from ref. 128. Copyright 2018, Wiley-VCH.

quantum dot (MWCNT/NCQD)-coated separator applied in Li–S batteries.[129] The cells showed a relatively high initial discharge capacity of 1330.8 mA h g$^{-1}$ and retained 507.9 mA h g$^{-1}$ after 1000 cycles at 0.5C.

Although Li–S batteries are regarded as a new kind of energy storage device because of their remarkable theoretical energy density, some issues, such as the low conductivity and the large volume variation of sulfur, as well as the formation of polysulfides during cycling, are yet to be addressed before Li–S batteries can become an actual reality. CDs with rich oxygen-rich functional groups are beneficial not only for increasing Li$^+$ ion conductivity around the solid–electrolyte interface but also for providing abundant absorption sites that could effectively restrain the polysulfide dissolution. CDs offer a novel way to tailor the oxygen-rich functional groups of nanosized carbon and improve sulfur utilization and stability for applications in Li–S batteries.

### 3.6 Metal–air batteries

Metal–air batteries are considered as a more effective and practical device for sustainable electric power supply given their low production cost and environmental friendliness derived from the use of metals as anodes and air-electrodes as cathodes.[130–133] However, the unsatisfactory service performance of metal–air batteries is significantly generated by the sluggish kinetics of the ORR/OER on the cathodes during charge/discharge processes.

Therefore, electro-catalysts with bi-functions are desired to overcome the activation energy and accelerate the reactions during the charging–discharging cycles. Graphene, CNTs, porous carbon and other carbon-based materials can only offer a good electron transfer path, enough surface area and so on.[134–136] When CDs are doped, these nanostructures will have abundant defective edges so as to be more promising for advanced ORR/OER catalysts. In previous years, many research achievements have proved their high catalytic activity and stability in the ORR or OER. Recently, some researchers have tried to use them in efficient air-electrodes with high-performance, such as lower charge voltage, higher discharge voltage and longer life span.

Zinc–air batteries (ZABs) are composed of zinc anodes, alkaline electrolytes and air electrodes with active materials.[137] Among different parts of ZABs, air electrodes play the most important role, and related research mainly focuses on this. As mentioned above, CDs can be good candidates to enhance the ORR/OER; therefore, they are also worth being used in related catalytic reactions. There are two typical examples in ZABs. Wang et al. tried to use defect-rich CDs/nitrogen doped graphene composites as efficient air-electrodes for aqueous zinc–air batteries.[138] As shown in Fig. 15a, through hydrothermal-activation-calcination methods, CDs (the black dots circled with red circles) could exist in the graphene matrix, where the defect-rich CDs provided more active sites to accelerate the ORR process. Proved by linear sweep voltammetry (LSV) tests (Fig. 15b), graphene samples with CDs showed higher half-wave potentials (graphene without CDs as the blank), even higher than commercial Pt/C. Accordingly, ZABs made from the optimal composite exhibited a higher power density. Another significant research was conducted by Zhang et al.[139] In this research, CDs were added in the preparation of Co$_9$S$_8$/N,S-codoped carbon (NSC) composites, and played a key role in distributing Co$_9$S$_8$ nanoparticles in the matrix uniformly (Fig. 15e and f). Moreover, CDs also enhanced the specific surface area and the electrical conductivity of the final products simultaneously. The optimal Co$_9$S$_8$/CD@NSC exhibited excellent ORR and OER bifunctional catalytic performance and good long-term stability, with a half-wave potential of 0.84 V vs. reversible hydrogen electrode (RHE) for the ORR and a low potential of 1.62 V vs. RHE at 10 mA cm$^{-2}$ (Fig. 15g), which outperformed the common Pt/C or RuO$_2$ commercial catalysts. As the cathode of ZABs, the Co$_9$S$_8$/CD@NSC catalyst also displayed superior activity, in terms of high platform of discharge (ORR), low platform of charge (OER) and high peak power density (92.7 mW cm$^{-2}$), which are all far better than those of Pt/C + RuO$_2$ mixture catalysts (Fig. 15h and i). At the same time, such ZAB devices showed a great cycling span of over 125 h at 10 mA cm$^{-2}$ without an obvious polarization process, which was also related to the contribution of CDs in constructing a stable and active surficial structure (Fig. 15j).

Apart from ZABs, CD-like materials were also employed in lithium–oxygen batteries (Li–O$_2$ batteries). According to the research work of Liu and his group, carbon-dotted defective CoO showed great potential in bifunctional cathode catalysts of Li–O$_2$ batteries.[140] In comparison with the commercial or

This journal is © The Royal Society of Chemistry and the Chinese Chemical Society 2020

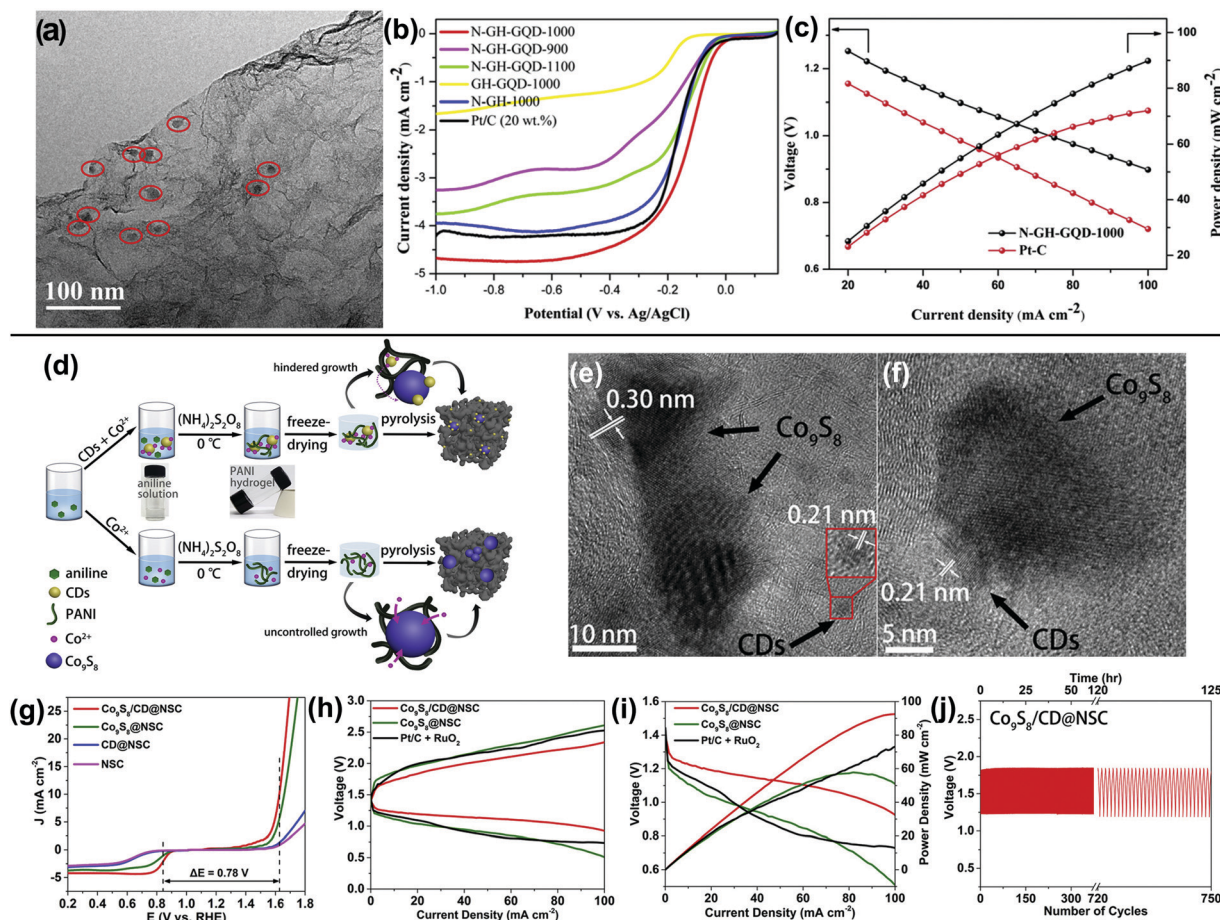*Mater. Chem. Front.*, 2020, **4**, 729–749 | **743**

Fig. 15 (a) TEM images of GQD/graphene composites (N-GH-GQD-1000); (b) linear sweep voltammetry (LSV) curves of different samples with a scan rate of 5 mV s$^{-1}$; (c) the discharge voltage profiles of N-GH-GQD-1000 and Pt–C. Reprinted with permission from ref. 138. Copyright 2017 Elsevier. (d) Schematic illustration of the preparation procedures of final products with ($Co_9S_8$/CD@NSC) or without ($Co_9S_8$@NSC) CDs; (e and f) HRTEM pictures of $Co_9S_8$/CD@NSC with lattices of both $Co_9S_8$ and CDs; (g) polarization curves of different studied samples in the overall potential range of the ORR and OER ($\Delta E = E_{1/2} - E_{j=10}$); (h) discharge–charge polarization curves of $Co_9S_8$/CD@NSC, $Co_9S_8$@NSC and Pt/C-$RuO_2$ mixtures, respectively; (i) discharge curves and the corresponding power density plots of the samples in Fig. 16(h); (j) potential profiles against time of the ZAB discharge/charge cycling tests with a current density of 10 mA cm$^{-2}$ and a duration time of 10 min for each cycle, employing sample $Co_9S_8$/CD@NSC. Reprinted with permission from ref. 139. Copyright 2019, American Chemical Society.

oxygen-vacancies-only CoO, defective CoO with carbon dot like structures showed better performances in terms of the initial capacity, rate capability and cycling stability (Fig. 16a–c). Fig. 16f schematically illustrates the function of the carbon-dotted species in the ORR and OER processes. Oxygen vacancies in CoO can enhance the mobility of electrons and Li$^+$ and bind to $O_2$ and $Li_2O_2$ as active sites. Further, carbon-dotted species not only had a high ORR activity but also improved the electrical conductivity of CoO and stabilized oxygen vacancies. Therefore, more stable oxygen vacancies could maximize the effects, including enhancing the mobility of electrons and Li$^+$ and binding to $O_2$ and $Li_2O_2$ as active sites, which synergistically enhanced the electrochemical performances of CoO/C-dotted species as catalysts for Li–$O_2$ batteries.

Besides Li–$O_2$/air batteries and ZABs, recent studies also recognized the role played by CDs in lithium–$CO_2$ (Li–$CO_2$) batteries. A typical work of Dai and co-workers showed graphene quantum dots (GQDs) supported by graphene

nanoribbons (GNRs) as a high-performance metal free catalyst for Li–$CO_2$ batteries.[130] Fig. 16g and h reveal that GQDs of 5–10 nm in size were uniformly dispersed on the planar surface of holey graphene sheets. The high-resolution (HR)-TEM image of the GQDs (inset, Fig. 16h) showed a clear lattice spacing of 3.5 Å, corresponding to the (002) plane of GQDs. The most obvious effect of such structures was revealed by contact angle tests. As shown in Fig. 16i and j, anchoring GQDs onto the graphene basal plane caused an obvious enhancement of the surface hydrophilicity, reflected by a decrease in the contact angle from 29° for the pure graphene based electrode to nearly 0° for the optimal sample (j) based electrode, which was related to the surface modification with oxygen-rich GQDs and the surface roughening caused by GQDs. The hydrophilic surface made the optimal composite highly miscible with the electrolyte solution, facilitating charge transfer across the electrode–electrolyte interface during the charge–discharge processes. Therefore, the sample decorated with GQDs exhibited a lower
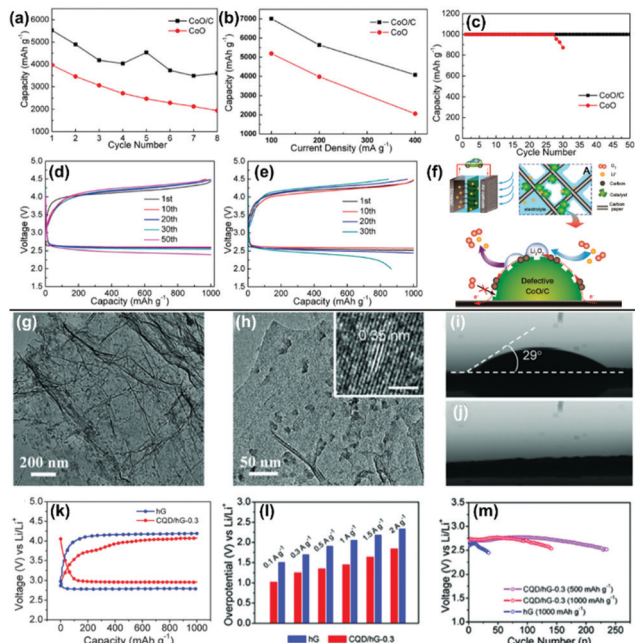
**Fig. 16** (a) Full cycling stability of CoO/C-dots and CoO-based air-electrodes at a current density of 0.2 A g$^{-1}$; (b) initial capacity comparison of the above samples at different current densities; (c) the cycle performances of the above cathodes with a limited capacity of 1000 mA h g$^{-1}$ at 0.2 A g$^{-1}$; (d and e) the discharge–charge curves of CoO/C-dots and CoO-based air-electrodes at different cycles, respectively; (f) scheme of the synergetic effects of the dotted carbon and oxygen vacancies in CoO/C-dots on the ORR and OER (above). Reproduced with permission from ref. 140. Copyright 2016 American Chemical Society; (g and h) TEM and HRTEM images of the CQDs-holey graphene composites (CQD/hG-0.3); (i and j) contact angle for holey graphene (hG) and composites in 1 M LiTFSI/DMSO + 0.3 M LiNO$_3$ solution; (k) the first discharge–charge curves for the Li–CO$_2$ batteries based on hG and CQD/hG composite catalysts; (l) overpotentials of the above samples at different current densities and (m) long-term stability. Reproduced with permission from ref. 130. Copyright 2018, Wiley-VCH.



**Fig. 17** (a) Scheme for the preparation of CDs/GF. (b) Laser scanning confocal microscopy tests of CDs/GF. SEM and HRTEM images of (c and e) GF and (d and f) CDs/GF. (g) Raman spectra of GF and CDs/GF. (h) Wettability test of the GF and CDs/GF. CV and Nyquist plots of different electrodes in the (i and j) positive electrolyte and the (k and l) negative electrolyte. (m) Digital images, (n) rate performance, and (o) Nyquist plots of VFBs assembled with different electrodes. (p) Cycling performance of the VFB assembled with the CDs/GF electrode. Reprinted with permission from ref. 153. Copyright 2017 Royal Society of Chemistry.

discharge/charge voltage gap (Fig. 16k), lower overpotential at large current densities (Fig. 16l) and longer life span (Fig. 16m).

Indeed, CDs with substantial edge defects and quantum confinement have attracted extensive attention as efficient air electrodes. However, surficial groups or defects of CDs are mainly based on some specific nonmetal elements, such as oxygen, nitrogen, *etc.* More than that, transition metal elements such as iron or cobalt and others may be better candidates for doping. Thus, it is an attractive option to conduct related research for new generation doped CDs as robust catalysts for metal–air batteries.

### 3.7 Flow batteries

Flow batteries, especially vanadium flow batteries (VFBs), are regarded as a type of most promising device for large-scale energy storage due to their huge capacity, fast response, long cycling span and low maintenance cost.[141–145] The performances of VFBs are highly dependent on some core components such as the electrodes, separators and electrolytes. Among them, the most crucial issue exists with electrodes due to their low

electrochemical activity. Both carbon felt (CF) and graphite felt (GF) will directly cause polarization of redox reactions or corrosion, which leads to power loss of VFBs.[146–148] Thus, it is important to develop novel electrode materials with high electro-catalytic activity, high power density and corrosion resistance for VFBs.

Generally, carbon-based electrode materials are promising candidates in VFBs, which include N-doped porous carbon, nanofibers, CNTs or graphene for their high specific surface area and good conductivity.[149–152] Although these carbon-based materials can exhibit enhanced catalytic activity toward vanadium redox reactions, the power densities of VFBs are still unsatisfactory. Inspired by CDs with high electrocatalytic activity and stable structures, Xi and his group tried for the first time to prepare carbon dot-decorated graphite felt (CDs/GF) electrodes (Fig. 17a).[153] These novel electrode architectures exhibited advantages as follows: (1) enhancement of electrolyte accessibility (Fig. 17h); (2) enhancement of the reversibility of electrochemical reactions, reduction of the charge transfer resistance and improvement of the rate as well as cycling stability in VFBs (Fig. 17i–p); (3) increase of the electrolyte utilization and power density of VFBs. Corresponding reasons include (1) large specific surface area and abundant surface edge/defects of CDs would improve the catalytic activity; (2) excellent water solubility of CDs would facilitate the contact between the electrode and electrolyte; (3) stable structure of CDs ensures VFBs are robust during long-term cycling.

It should be noted that the research of CDs in flow batteries is still at the early stage. For example, apart from carbon-based

This journal is © The Royal Society of Chemistry and the Chinese Chemical Society 2020

*Mater. Chem. Front.*, 2020, **4**, 729–749 | **745**

**Fig. 18** Development and prospects of CDs in electrochemical applications.

materials, metal oxide-based electrodes with high catalytic activity are also a good choice for flow batteries. However, these materials are hindered by their high price, easy passivation or corrosion. Therefore, how to use CDs to solve the above issues is also worth investigating.

## 4. Summary and outlook

We have briefly overviewed the different types, preparation and electrochemical properties of CDs, and their emerging potential for energy storage applications based on the cutting-edge research outputs over the last decade. Their unique quantum size effects, good electrical conductivity, rich surface functional groups, various defects and edges endow CDs with a dominating role in the electrochemical performance of many electrochemical storage devices including supercapacitors, Li/Na/K-ion batteries, Li–S batteries, metal–air batteries, flow batteries, *etc.* (Fig. 18). It is technically feasible to employ CDs either as building units to construct an electrode, or as additives to combine with other materials to exhibit synergistic effects. In addition, CDs could be a key component in composite materials to carry out particular functions, such as a surface protector, a corrosion inhibitor in electrolytes, and a buffer for retaining volume stability during charging/discharging cycles. To explore such functional abilities of CDs, a comprehensive understanding of the basic science of CDs and well-designed structures beforehand are essential. However, research on CDs for electrochemical applications is at the early stage now, and is facing two major challenges. One is developing large-scale synthetic routes for CDs. Such routes must be controllable, repeatable and cost-effective, because the practical energy storage devices require plenty of electrode materials. The other challenge is to obtain uniform CDs with exact structures, including their crystallinity, size, defects and surface states, so that their electrochemical properties can be tuned and predicted for practical applications. In most reports, the synthesized CDs are actually mixtures containing amorphous carbon, oligomers, precursors and other impurities, which render the composite electrodes unstable, and the experimental results in different research papers are often incomparable. Nevertheless, CDs have evidently exhibited their promising potential in a wide range of electrochemical applications. We believe that the extraordinary physical–chemical properties of CDs will inspire exciting and solid advancements towards practical deployment of high-performance energy storage facilities in the near future.

## Conflicts of interest

There are no conflicts to declare.

## Acknowledgements

## Notes and references

1 Y. Zhai, Y. Dou, D. Zhao, P. F. Fulvio, R. T. Mayes and S. Dai, *Adv. Mater.*, 2011, **23**, 4828–4850.

2 Y. Zhu, Z. Wu, M. Jing, H. Hou, Y. Yang, Y. Zhang, X. Yang, W. Song, X. Jia and X. Ji, *J. Mater. Chem. A*, 2014, **3**, 866–877.

3 J. C. Li, P. X. Hou and C. Liu, *Small*, 2017, **13**, 1702002.

4 Y. Jiao, D. Han, L. Liu, L. Ji, G. Guo, J. Hu, D. Yang and A. Dong, *Angew. Chem., Int. Ed.*, 2015, **54**, 5727–5731.

5 X. Wei, H. Zou and S. Gao, *Carbon*, 2017, **123**, 471–480.

6 J. Xu, Y. Dou, Z. Wei, J. Ma, Y. Deng, Y. Li, H. Liu and S. Dou, *Adv. Sci.*, 2017, **4**, 1700146.

7 H. Hou, X. Qiu, W. Wei, Z. Yun and X. Ji, *Adv. Energy Mater.*, 2017, **7**, 1602898.

8 H. Zheng, Z. Yang, F. Kang and M. Inagaki, *J. Mater. Chem. A*, 2017, **5**, 470–496.

9 P. Simon and Y. Gogotsi, *Acc. Chem. Res.*, 2013, **46**, 1094–1103.

10 Y. Liang, Y. Jing, S. Gheytani, K. Y. Lee, P. Liu, A. Facchetti and Y. Yao, *Nat. Mater.*, 2017, **16**, 841–848.

11 J. Wei, C. Ding, P. Zhang, H. Ding, X. Niu, Y. Ma, C. Li, Y. Wang and H. Xiong, *Adv. Mater.*, 2019, **31**, 1806197.

12 RnRMarketResearch.com, http://www.rnrmarketresearch.com.

13 alibaba.com, 2016, http://www.alibaba.com.

14 X. Xu, R. Ray, Y. Gu, H. J. Ploehn, L. Gearheart, K. Raker and W. A. Scrivens, *J. Am. Chem. Soc.*, 2015, **126**, 12736–12737.

15 X. Li, M. Rui, J. Song, Z. Shen and H. Zeng, *Adv. Funct. Mater.*, 2015, **25**, 4929–4947.

16 Y. Zhu, X. Ji, C. Pan, Q. Sun, W. Song, L. Fang, Q. Chen and C. E. Banks, *Energy Environ. Sci.*, 2013, **6**, 3665–3675.

17 D. Chao, C. Zhu, X. Xia, J. Liu, X. Zhang, J. Wang, P. Liang, J. Lin, H. Zhang and Z. X. Shen, *Nano Lett.*, 2015, **15**, 565.

18 J. M. Chabu, K. Zeng, G. Jin, M. Zhang, Y. Li and Y.-N. Liu, *Mater. Chem. Phys.*, 2019, **229**, 226–231.

19 C. Qing, H. Yue, H. Chuangang, C. Huhu, Z. Zhipan, S. Huibo and Q. Liangti, *Phys. Chem. Phys. Chem.*, 2014, **16**, 19307–19313.

20 S. Zhu, Y. Song, X. Zhao, J. Shao, J. Zhang and B. Yang, *Nano Res.*, 2015, **8**, 355–381.

21 H. Ding, S. B. Yu, J. S. Wei and H. M. Xiong, *ACS Nano*, 2016, **10**, 484–491.

22 G. Jin, M. Zhu, H. Hui, L. Yang and Z. Kang, *Inorg. Chem. Front.*, 2017, **4**, 1963–1986.

23 H. Ding, J. Wei and H. Xiong, *Nanoscale*, 2014, **6**, 13817–13823.

24 P. Zhang, J. Wei, X. Chen and H. Xiong, *J. Colloid Interface Sci.*, 2019, **537**, 716–724.

25 C. Hu, M. Li, J. Qiu and Y. Sun, *Chem. Soc. Rev.*, 2019, **48**, 2315–2337.

26 K. Manpreet, K. Manmeet and V. K. Sharma, *Adv. Colloid Interface Sci.*, 2018, **259**, 44–64.

27 J. Wei, H. Ding, P. Zhang, Y. Song, J. Chen, Y. Wang and H. Xiong, *Small*, 2016, **12**, 5927–5934.

28 X. Wei, S. Wan and S. Gao, *Nano Energy*, 2016, **28**, 206–215.

29 X. Wei, Y. Li and S. Gao, *J. Mater. Chem. A*, 2017, **5**, 181–188.

30 Y. Wang, Y. Song and Y. Xia, *Chem. Soc. Rev.*, 2016, **45**, 5925–5950.

31 C. Zhang, Y. Wei, P. Cao and M. Lin, *Renewable Sustainable Energy Rev.*, 2018, **82**, 3091–3106.

32 G. Wang, L. Zhang and J. Zhang, *Chem. Soc. Rev.*, 2012, **41**, 797–828.

33 A. G. Pandolfo and A. F. Hollenkamp, *J. Power Sources*, 2006, **157**, 11–27.

34 F. Béguin, V. Presser, A. Balducci and E. Frackowiak, *Adv. Mater.*, 2014, **26**, 2283.

35 Q. Wu, Y. Xu, Z. Yao, A. Liu and G. Shi, *ACS Nano*, 2010, **4**, 1963–1970.

36 L. Chen, X. Zhang, H. Liang, M. Kong, Q. Guan, P. Chen, Z. Wu and S. Yu, *ACS Nano*, 2012, **6**, 7092–7102.

37 H. Pan, J. Li and Y. P. Feng, *Nanoscale Res. Lett.*, 2010, **5**, 654–668.

38 C. Liu, Z. Yu, D. Neff, A. Zhamu and B. Jang, *Nano Lett.*, 2010, **10**, 4863–4868.

39 Q. Ke and J. Wang, *J. Materiomics*, 2016, **2**, 37–54.

40 M. Khattak, Z. A. Ghazi, B. Liang, N. A. Khan, A. Iqbal, L. Li and Z. Tang, *J. Mater. Chem. A*, 2016, **4**, 16312–16317.

41 I. Yoshikazu, C. Christos, M. V. Nardi, K. Norbert, K. U. Mathias, S. Hermann and M. L. Klaus, *J. Am. Chem. Soc.*, 2015, **137**, 7678.

42 M. Yu, D. Lin, H. Feng, Y. Zeng, Y. Tong and X. Lu, *Angew. Chem., Int. Ed.*, 2017, **56**, 5454.

43 M. Yang, Y. Zhong, J. Ren, X. Zhou, J. Wei and Z. Zhou, *Adv. Energy Mater.*, 2015, **5**, 1500550.

44 Y. Qing, Y. Jiang, H. Lin, L. Wang, A. Liu, Y. Cao, R. Sheng, Y. Guo, C. Fan and Z. Fan, *J. Mater. Chem. A*, 2019, **7**, 6021–6027.

45 K. Lee, H. Lee, Y. Shin, Y. Yoon, D. Kim and H. Lee, *Nano Energy*, 2016, **26**, 746–754.

46 C. Hu, K. Chang, M. Lin and Y. Wu, *Nano Lett.*, 2006, **6**, 2690–2695.

47 S. Chen, J. Zhu, X. Wu, Q. Han and X. Wang, *ACS Nano*, 2010, **4**, 2822.

48 G. A. Snook, P. Kao and A. S. Best, *J. Power Sources*, 2011, **196**, 1–12.

49 Z. Zhao and Y. Xie, *J. Power Sources*, 2017, **337**, 54–64.

50 M. Sanjoy, R. Utpal and M. Sudip, *Chem. Commun.*, 2015, **51**, 12365.

51 J. Xuan, J. Li, H. Yang, L. L. Cao, E. Zhang and Z. Liang, *Carbon*, 2017, **114**, 533–543.

52 H. Lv, Y. Yue, Q. Xu, L. H. Liu, Y. G. Wang and Y. Xia, *J. Power Sources*, 2018, **398**, 167–174.

53 D. P. Dubal, O. Ayyad, V. Ruiz and P. Gomez-Romero, *Chem. Soc. Rev.*, 2015, **44**, 1777–1790.

54 W. Zuo, R. Li, C. Zhou, Y. Li, J. Xia and J. Liu, *Adv. Sci.*, 2017, **4**, 1600539.

55 P. Thounthong, S. Raël and B. Davat, *J. Power Sources*, 2009, **193**, 376–385.

56 H. Kim, M. Y. Cho, M. H. Kim, K. Y. Park, H. Gwon, Y. Lee, K. C. Roh and K. Kang, *Adv. Energy Mater.*, 2013, **3**, 1500–1506.

57 Q. Wang, Z. Wen and J. Li, *Adv. Funct. Mater.*, 2010, **16**, 2141–2146.

58 B. Li, F. Dai, Q. Xiao, L. Yang, J. Shen, C. Zhang and M. Cai, *Energy Environ. Sci.*, 2016, **9**, 102–106.

59 J. Yan, Z. Fan, S. Wei, G. Ning, W. Tong, Z. Qiang, R. Zhang, L. Zhi and W. Fei, *Adv. Funct. Mater.*, 2012, **22**, 2632–2641.

60 L. Shen, J. Wang, G. Xu, H. Li, H. Dou and X. Zhang, *Adv. Energy Mater.*, 2015, **5**, 1400977.

61 J. M. Tarascon and M. Armand, *Nature*, 2001, **414**, 359–367.

62 Y. Xue, Z. Qin, Z. Tao and F. Lei, *ChemNanoMat*, 2017, **3**, 352–361.

63 Y. Xue, Q. Zhang, W. Wang, H. Cao, Q. Yang and L. Fu, *Adv. Energy Mater.*, 2017, **7**, 1602684.

64 J. Pang, A. Bachmatiuk, Y. Yin, B. Trzebicka and M. H. Rummeli, *Adv. Energy Mater.*, 2018, **8**, 1702093.

65 M. Winter, J. O. Besenhard, M. E. Spahr and P. Novak, *Cheminform*, 1998, **10**, 725–763.

66 Y. Shaohorn, L. Croguennec, C. Delmas, E. C. Nelson and M. A. O'Keefe, *Nat. Mater.*, 2003, **2**, 464.

67 X. Li, L. Jian, X. Meng, Y. Tang, M. N. Banis, J. Yang, Y. Hu, R. Li, C. Mei and X. Sun, *J. Power Sources*, 2014, **247**, 57–69.

68 K. Mizushima, P. C. Jones, P. J. Wiseman and J. B. Goodenough, *Mater. Res. Bull.*, 2015, **15**, 783–789.

69 L. Qie, W. Chen, Z. Wang, Q. Shao, X. Li, L. Yuan, X. Hu, W. Zhang and Y. Huang, *Adv. Mater.*, 2012, **24**, 2047–2050.

70 S. W. Kim, D. H. Seo, X. Ma, G. Ceder and K. Kang, *Adv. Energy Mater.*, 2012, **2**, 710–721.

71 M. Ge, J. Rong, F. Xin and C. Zhou, *Nano Lett.*, 2012, **12**, 2318–2323.

72 W. Zhang, J. Hu, Y. Guo, S. Zheng, L. Zhong, W. Song and L. Wan, *Adv. Mater.*, 2010, **20**, 1160–1165.

73 J. Sun, G. Zheng, H. W. Lee, N. Liu, H. Wang, H. Yao, W. Yang and Y. Cui, *Nano Lett.*, 2012, **14**, 4573–4580.

74 H. Wu, J. Chen, H. Hng and X. Lou, *Nanoscale*, 2012, **4**, 2526–2542.

This journal is © The Royal Society of Chemistry and the Chinese Chemical Society 2020

*Mater. Chem. Front.*, 2020, **4**, 729–749 | 747

75 Z. Wang, L. Zhou and X. W. Lou, *Cheminform*, 2012, **24**, 1903–1911.

76 Y. Wang, H. Liu, K. Wang, H. Eiji, Y. Wang and H. Zhou, *J. Mater. Chem. A*, 2009, **19**, 6789–6795.

77 C. Yang, X. Ma, X. Cui and Z. Jiang, *J. Power Sources*, 2016, **302**, 233–239.

78 J. Zhou, J. Qin, X. Zhang, C. Shi, E. Liu, J. Li, N. Zhao and C. He, *ACS Nano*, 2015, **9**, 3837–3848.

79 D. Wang, Y. Liu, M. Xing, Y. Wei and C. Gang, *J. Mater. Chem. A*, 2017, **5**, 21370–21377.

80 X. Zhao, D. Xia and K. Zheng, *J. Alloys Compd.*, 2012, **513**, 460–465.

81 M. Jing, J. Wang, H. Hou, Y. Yang, Y. Zhang, C. Pan, J. Chen, Y. Zhu and X. Ji, *J. Mater. Chem. A*, 2015, **3**, 16824–16830.

82 X. Yin, C. Zhi, W. Sun, L. P. Lv and Y. Wang, *J. Mater. Chem. A*, 2019, **7**, 7800–7814.

83 M. Wu, H. Chen, L. Lv and Y. Wang, *Chem. Eng. J.*, 2019, **373**, 985–994.

84 C. Zhu, D. Chao, S. Jing, I. M. N. Bacho and J. F. Hong, *Adv. Mater. Interfaces*, 2015, **2**, 1400499.

85 Y. Zhang, K. Zhang, K. Jia, G. Liu, S. Ren, K. Li, X. Long, M. Li and J. Qiu, *Fuel*, 2019, **241**, 646–652.

86 P. Roy and S. K. Srivastava, *J. Mater. Chem. A*, 2015, **3**, 2454–2484.

87 L. Ji, Z. Lin, M. Alcoutlabi and X. Zhang, *Energy Environ. Sci.*, 2011, **4**, 2682–2699.

88 W. Wen and J. M. Lee, *J. Mater. Chem. A*, 2014, **2**, 1589–1626.

89 F. Khan, M. Oh and J. H. Kim, *Chem. Eng. J.*, 2019, **369**, 1024–1033.

90 R. Li, Y. Jiang, X. Zhou, Z. Li, Z. Gu, G. Wang and J. Liu, *Electrochim. Acta*, 2015, **178**, 303–311.

91 Y. Yang, X. Ji, M. Jing, H. Hou and C. E. Banks, *J. Mater. Chem. A*, 2015, **3**, 5648–5655.

92 I. S. Riyanto, K. Bindumadhavan, P. Chang and R. Doong, *Front. Chem.*, 2019, **7**, 116.

93 H. Li, T. Jin, X. Chen, Y. Lai, Z. Zhang, W. Bao and L. Jiao, *Adv. Energy Mater.*, 2018, **8**, 1801418.

94 X. Xiang, K. Zhang and J. Chen, *Cheminform*, 2015, **46**, 5343–5364.

95 T. Song, H. Chen, Z. Li, Q. Xu, H. Liu, Y. Wang and Y. Xia, *Adv. Funct. Mater.*, 2019, **29**, 1900535.

96 W. Shen, C. Wang, Q. Xu, H. Liu and Y. Wang, *Adv. Energy Mater.*, 2015, **5**, 1400982.

97 N. Zhang, X. Han, Y. Liu, X. Hu, Q. Zhao and J. Chen, *Adv. Energy Mater.*, 2015, **5**, 1401123.

98 G. Xu, Z. Chen, G. Zhong, Y. Liu, Y. Yang, T. Ma, Y. Ren, X. Zuo, X. Wu and X. Zhang, *Nano Lett.*, 2016, **16**, 3955–3965.

99 E. Irisarri, A. Ponrouch and M. Palacin, *J. Electrochem. Soc.*, 2015, **162**, A2476–A2482.

100 Y. Wang, S. Chou, H. Liu and S. Dou, *Carbon*, 2013, **57**, 202–208.

101 J. Yang, X. Zhou, D. Wu, X. Zhao and Z. Zhou, *Adv. Mater.*, 2017, **29**, 1604108.

102 H. Hou, C. E. Banks, M. Jing, Y. Zhang and X. Ji, *Adv. Mater.*, 2015, **27**, 7861–7866.

103 Z. Liu, L. Zhang, L. Sheng, Q. Zhou, T. Wei, J. Feng and Z. Fan, *Adv. Energy Mater.*, 2018, **8**, 1802042.

104 M. Javed, A. N. S. Saqib, B. Ali, M. Faizan, D. A. Anang, Z. Iqbal and S. M. Abbas, *Electrochim. Acta*, 2019, **297**, 250–257.

105 T. Song, H. Chen, Q. Xu, H. Liu, Y.-G. Wang and Y. Xia, *ACS Appl. Mater. Interfaces*, 2018, **10**, 37163–37171.

106 Q. Wang, C. Zhao, Y. Lu, Y. Li, Y. Zheng, Y. Qi, X. Rong, L. Jiang, X. Qi and Y. Shao, *Small*, 2017, **13**, 1701835.

107 Z. Yan, L. Li, H. Shu, X. Yang, W. Hao, J. Tan, Z. Qian, Z. Huang and X. Wang, *J. Power Sources*, 2015, **274**, 8–14.

108 Y. Zhang, C. W. Foster, C. E. Banks, L. Shao, H. Hou, G. Zou, J. Chen, Z. Huang and X. Ji, *Adv. Mater.*, 2016, **28**, 9391–9399.

109 D. Kong, Y. Wang, S. Huang, Y. V. Lim, J. Zhang, L. Sun, B. Liu, T. Chen, P. V. Y. Alvarado and H. Y. Yang, *J. Mater. Chem. A*, 2019, **7**, 12751–12762.

110 M. S. Balogun, Y. Luo, F. Lyu, F. Wang, H. Yang, H. Li, C. Liang, M. Huang, Y. Huang and Y. Tong, *ACS Appl. Mater. Interfaces*, 2016, **8**, 9733.

111 N. Chaojiang, M. Jiashen, H. Chunhua, Z. Kangning, Y. Mengyu and M. Liqiang, *Nano Lett.*, 2014, **14**, 2873–2878.

112 D. Su, A. Mcdonagh, S. Z. Qiao and G. Wang, *Adv. Mater.*, 2017, **29**, 1604007.

113 J. C. Pramudita, D. Sehrawat, D. Goonetilleke and N. Sharma, *Adv. Energy Mater.*, 2017, **7**, 1602911.

114 S. Komaba, T. Hasegawa, M. Dahbi and K. Kubota, *Electrochem. Commun.*, 2015, **60**, 172–175.

115 W. Luo, J. Wan, B. Ozdemir, W. Bao, Y. Chen, J. Dai, H. Lin, Y. Xu, F. Gu and V. Barone, *Nano Lett.*, 2015, **15**, 7671–7677.

116 Z. Jian, W. Luo and X. Ji, *J. Am. Chem. Soc.*, 2015, **137**, 11566.

117 Z. Jian, Z. Xing, C. Bommier, Z. Li and X. Ji, *Adv. Energy Mater.*, 2016, **6**, 1501874.

118 K. Share, A. P. Cohn, R. Carter, B. Rogers and C. L. Pint, *ACS Nano*, 2016, **10**, 9738–9744.

119 Y. Zhang, L. Yang, Y. Tian, L. Li, J. Li, T. Qiu, G. Zou, H. Hou and X. Ji, *Mater. Chem. Phys.*, 2019, **229**, 303–309.

120 T. Li, X. Bai, U. Gulzar, Y. J. Bai, C. Capiglia, W. Deng, X. Zhou, Z. Liu, Z. Feng and R. Proietti Zaccaria, *Adv. Funct. Mater.*, 2019, **29**, 1901730.

121 A. Manthiram, Y. Fu and Y. S. Su, *Acc. Chem. Res.*, 2012, **46**, 1125–1134.

122 J. Wang, Y. S. He and J. Yang, *Adv. Mater.*, 2015, **27**, 569–575.

123 Y. Son, J. S. Lee, Y. Son, J. H. Jang and J. Cho, *Adv. Energy Mater.*, 2015, **5**, 1500110.

124 D. W. Wang, Q. Zeng, G. Zhou, L. Yin, L. Feng, H. M. Cheng, I. R. Gentle and Q. M. L. Gao, *J. Mater. Chem. A*, 2013, **1**, 9382–9394.

125 L. Ji, Z. H. Sun, L. Feng and H. M. Cheng, *Energy Storage Mater.*, 2016, **2**, 76–106.

126 M. Zhao, X. Liu, Q. Zhang, G. Tian, J. Huang, W. Zhu and W. Fei, *ACS Nano*, 2012, **6**, 10759–10769.

**748** | *Mater. Chem. Front.*, 2020, **4**, 729–749

This journal is © The Royal Society of Chemistry and the Chinese Chemical Society 2020

127 J. Park, J. Moon, C. Kim, H. K. Jin, E. Lim, J. Park, K. J. Lee, S. H. Yu, J. H. Seo and J. Lee, *NPG Asia Mater.*, 2016, **8**, e272.

128 Y. Hu, W. Chen, T. Lei, B. Zhou, Y. Jiao, Y. Yan, X. Du, J. Huang, C. Wu and X. Wang, *Adv. Energy Mater.*, 2019, **9**, 1802955.

129 P. Ying, J. Wei, Y. Wang and Y. Xia, *Adv. Energy Mater.*, 2018, **8**, 1702288.

130 Y. Jin, C. Hu, Q. Dai, Y. Xiao, Y. Lin, J. W. Connell, F. Chen and L. Dai, *Adv. Funct. Mater.*, 2018, **28**, 1804630.

131 F. Cheng and J. Chen, *Chem. Soc. Rev.*, 2012, **41**, 2172.

132 M. A. Rahman, X. Wang and C. Wen, *J. Electrochem. Soc.*, 2013, **160**, A1759–A1771.

133 J. S. Lee, T. K. Sun, R. Cao, N. S. Choi, M. Liu, K. T. Lee and J. Cho, *Adv. Energy Mater.*, 2011, **1**, 34–50.

134 Y. Eunjoo and Z. Haoshen, *ACS Nano*, 2011, **5**, 3020–3026.

135 H. Huang, W. Zhang, M. Li, Y. Gan, J. Chen and Y. Kuang, *J. Colloid Interface Sci.*, 2005, **284**, 593–599.

136 H. Cheng and K. Scott, *J. Power Sources*, 2010, **195**, 1370–1374.

137 J. Fu, Z. P. Cano, M. G. Park, A. Yu, M. Fowler and Z. Chen, *Adv. Mater.*, 2017, **29**, 1604685.

138 M. Wang, F. Jing, L. Hu, Y. Lai and Z. Liu, *Int. J. Hydrogen Energy*, 2017, **42**, 21305–21310.

139 P. Zhang, D. Bin, J. Wei, X. Niu, X. Chen, Y. Xia and H. Xiong, *ACS Appl. Mater. Interfaces*, 2019, **11**, 14085–14094.

140 G. Rui, Z. Li, X. Zhang, J. Zhang and X. Liu, *ACS Catal.*, 2015, **6**, 400–406.

141 B. Schwenzer, J. Zhang, S. Kim, L. Li, J. Liu and Z. Yang, *ChemSusChem*, 2011, **4**, 1388–1406.

142 C. Ding, H. Zhang, X. Li, T. Liu and F. Xing, *J. Phys. Chem. Lett.*, 2013, **4**, 1281–1294.

143 D. S. Aaron, Q. Liu, Z. Tang, G. M. Grim, A. B. Papandrew, A. Turhan, T. A. Zawodzinski and M. M. Mench, *J. Power Sources*, 2012, **206**, 450–453.

144 Z. Yuan, Y. Duan, H. Zhang, X. Li, H. Zhang and I. Vankelecom, *Energy Environ. Sci.*, 2016, **9**, 441–447.

145 M. Skyllas-Kazacos, G. Kazacos, G. Poon and H. Verseema, *Int. J. Energy Res.*, 2010, **34**, 182–189.

146 W. Wang and X. Wang, *Electrochim. Acta*, 2007, **52**, 6755–6762.

147 K. J. Kim, Y. J. Kim, J. H. Kim and M. S. Park, *Mater. Chem. Phys.*, 2011, **131**, 547–553.

148 B. Li, M. Gu, Z. Nie, Y. Shao, Q. Luo, X. Wei, X. Li, J. Xiao, C. Wang and V. Sprenkle, *Nano Lett.*, 2013, **13**, 1330–1335.

149 J. Ryu, M. Park and J. Cho, *J. Electrochem. Soc.*, 2016, **163**, A5144–A5149.

150 A. Fetyan, I. Derr, M. K. Kayarkatte, J. Langner, C. Roth, D. Bernsmeier and R. Kraehnert, *ChemElectroChem*, 2016, **2**, 2055–2060.

151 W. Li, J. Liu and C. Yan, *Carbon*, 2011, **49**, 3463–3470.

152 W. Li, J. Liu and C. Yan, *Carbon*, 2013, **55**, 313–320.

153 Y. Zhou, L. Liu, Y. Shen, L. Wu, L. Yu, F. Liang and J. Xi, *Chem. Commun.*, 2017, **53**, 7565–7568.

This journal is © The Royal Society of Chemistry and the Chinese Chemical Society 2020

*Mater. Chem. Front.*, 2020, **4**, 729–749 | **749**